

ORIGINAL ARTICLE

Assessing the economic impacts of a perfect storm of extreme weather, pandemic control, and export restrictions: A methodological construct

Yixin Hu^{1,2}  | Daoping Wang^{3,4}  | Jingwen Huo⁵  | Vicky Chemutai⁶ | Paul Brenton⁶ | Lili Yang¹  | Dabo Guan^{5,7} 

¹Department of Statistics and Data Science, Southern University of Science and Technology, Shenzhen, China

²School of Environmental Sciences, University of East Anglia, Norwich, UK

³Department of Computer Science and Technology, University of Cambridge, Cambridge, UK

⁴Centre for Nature and Climate, World Economic Forum, Geneva, Switzerland

⁵Department of Earth System Science, Tsinghua University, Beijing, China

⁶The World Bank, Washington, District of Columbia, USA

⁷The Bartlett School of Construction and Project Management, University College London, London, UK

Correspondence

Dabo Guan, Department of Earth System Science, Tsinghua University, Beijing 100084, China.
Email: guandabo@tsinghua.edu.cn

Abstract

This article investigates the economic impacts of a multi-disaster mix comprising extreme weather, such as flooding, pandemic control, and export restrictions, dubbed a “perfect storm.” We develop a compound-hazard impact model that improves on the ARIO model by considering the economic interplay between different types of hazardous events. The model considers simultaneously cross-regional substitution and production specialization, which can influence the resilience of the economy to multiple shocks. We build scenarios to investigate economic impacts when a flood and a pandemic lockdown collide and how these are affected by the timing, duration, and intensity/strictness of each shock. In addition, we examine how export restrictions during a pandemic impact the economic losses and recovery, especially when there is the specialization of production of key sectors. The results suggest that an immediate, stricter but shorter pandemic control policy would help to reduce the economic costs inflicted by a perfect storm, and regional or global cooperation is needed to address the spillover effects of such compound events, especially in the context of the risks from deglobalization.

KEYWORDS

compound hazard, disaster footprint, risk assessment, ARIO model

1 | INTRODUCTION

During the past year, the escalating COVID-19 pandemic appeared to have diverted attention away from the climate crisis (Selby & Kagawa, 2020; The Lancet Planetary Health, 2020), despite the fact that just a few years prior, the WHO had identified climate change as “the greatest threat to global health in the 21st century” (WHO, 2015). The year 2020 saw a number of climate disasters. It has been reported to have been the hottest year on record (Gohd, 2021). The dry and hot conditions fueled massive record-breaking wildfires across Australia, Siberia, and the United States. The 2020 Atlantic hurricane season was also the most active in recorded history (White, 2020). Devastating typhoons swamped the Indian subcontinent and Southeast Asia, whereas the Sahel and

Greater Horn regions of Africa experienced severe droughts (Boyle, 2020) and devastation from locust swarms linked to climate change (UNEP, 2020). Early 2021 also saw the Swiss Alps develop an orange layer caused by heavy sandstorms from the Sahara Desert, the widest reach recorded in recent years (BBC News, 2021).

Several aspects of signaling deglobalization have been at play in recent years. The 2020 World Development Report reports that growth in global value chains has flattened (World Bank, 2019). The year 2020 saw increasing trade tensions, especially in relations between the United States and China, as well as the UK withdrawing from the EU, but also in some of the responses by governments to the pandemic. Indeed, some have argued that the pandemic has further fueled the process of deglobalization (Oxford Analytica, 2020; Shahid,

This is an open access article under the terms of the [Creative Commons Attribution](https://creativecommons.org/licenses/by/4.0/) License, which permits use, distribution and reproduction in any medium, provided the original work is properly cited.

© 2023 The Authors. *Risk Analysis* published by Wiley Periodicals LLC on behalf of Society for Risk Analysis.

2020). A number of countries have responded by introducing export restrictions on critical medical equipment and food and even on vaccines (Eaton, 2021; Espitia et al., 2020). This raises the issue of whether restrictive trade policy measures can undermine effective responses when climate and pandemic crises collide to create a perfect storm (Mahul & Signer, 2020).

The collision of climate extremes, pandemic control, and export restrictions creates a triple or compound event. The concept of “compound event” was originally used in climatic research and defined as the “combination of multiple drivers and/or hazards that contributes to societal or environmental risk” (AghaKouchak et al., 2020; Field et al., 2012; Hao et al., 2013; Leonard et al., 2014; Zscheischler et al., 2018). Unable to foresee such a globally explosive outbreak of the coronavirus, those studies were mainly focused on the co-occurrence of multiple dependent climatic hazards. Only very recently have researchers begun to incorporate the coexistence of biological hazards. As the pandemic and global warming continue, civil society will see a growing probability of collisions between coronavirus surges and climate crises (Phillips et al., 2020) in tandem with other global issues, such as deglobalization or intensifying trade tensions, following recent trends. Countermeasures against one crisis may jeopardize the effects against another and ultimately exacerbate the negative impacts of both (Ishiwatari et al., 2020; Salas et al., 2020; Selby & Kagawa, 2020). As a result, scholars have advocated for a comprehensive and holistic multi-hazard approach of disaster management that considers all possible hazards together with compound ones in the post-pandemic world (Chondol et al., 2020). Hariri-Ardebili (2020) proposed a multi-risk assessment tool to qualitatively study the hybrid impacts of compound-hazard situations on healthcare systems, whereas Shen et al. (2021) provided a tool to assess the compound risk from flooding and COVID-19 at the county level across the United States. Beyond these, researchers also developed optimization models to study the effectiveness of evacuation strategies in risk control when floods intersect with a pandemic (Pei et al., 2020; Tripathy et al., 2021).

An important aspect of risk management is to assess the economic consequences of hazardous events (Laframboise & Loko, 2012); however, this has been seldom touched upon so far in compound-hazard research. Typically, in single-hazard research, economic models, such as input–output (IO) and computable general equilibrium models, provide quantitative tools to evaluate the economic footprint of disruptive events (Botzen et al., 2019). Metrics related to disaster-induced economic damages, both direct and indirect,¹ are developed to inform cost-benefit decisions in disaster preparedness investment (ESCAP, 2019). With abundant studies focused on climate extremes (Hallegatte, 2008, 2014; Koks

et al., 2015; Koks & Thissen, 2016; Lenzen et al., 2019; Mendoza-Tinoco et al., 2020; Oosterhaven & Többen, 2017; Willner et al., 2018; Xia et al., 2018; Zeng et al., 2019), only a few have started studying biological hazards like the COVID-19 pandemic (Guan et al., 2020; McKibbin & Fernando, 2020). Even fewer studies have looked into the economic aspects of compound events. Zeng and Guan (2020) constructed an IO-based flood footprint model to quantify the combined indirect economic impacts of successive flood events. However, the interaction between pandemic control and flood responses is different from that between two flood events. Flood events are usually sudden or rapid onset events that require immediate emergency measures (Bubeck et al., 2017; Johnstone & Lence, 2009), whereas the pandemic lasts for longer periods, and the corresponding control measures could be of various durations and coincide with different flood periods. A focus on measures to prevent coronavirus transmission can result in inadequate response toward flood disasters (Ishiwatari et al., 2020) and constrain the economic flows required by post-flood recovery, aggravating the impact of the flood. Similar perspectives are suggested by Swaisgood (2020) that the economic consequences of such compound events are underestimated if the interplay between individual hazards is not considered. The compound effects of natural and pandemic hazards increase the complexity of economic consequences, which cannot be addressed by traditional single-hazard assessment techniques.

Given the current research gap, we propose a multiregional compound-hazard approach to assess the short-term economic impacts resulting from triple shocks of pandemic control, flooding, and export restrictions. The model, which is constructed under the ARIO-Inventory framework (Hallegatte, 2014), considers not only the economic-wise interplay between different types of negative shocks but also the possibility of cross-regional substitution and production specialization. We build scenarios on a hypothetical global economy consisting of four regions and five sectors where hazardous events with different durations and intensities collide at different spatial and temporal scales. We then use this approach to explore specific scenarios to understand the role of trade in disaster recovery during compound climate and health crises. We look at how export restrictions and the extent of production specialization influence the magnitude of economic losses.

Our study provides consistent and comparable loss metrics with single-hazard analysis and can be generalized to various types of compound events. This would support the formation of an integrated risk management strategy, including compound hazards, and the fulfillment of the mitigation and adaptation targets in the Paris Agreement and Sendai Framework for Disaster Risk Reduction (UNFCCC, 2015; UNISDR, 2015).

2 | METHODS AND DATA

Our compound-hazard impact model stems from the ARIO-Inventory model that introduces inventory dynamics and

¹ Direct damages refer to damages to humans, physical assets (e.g., buildings and infrastructure), and any other elements due to direct contact with disasters, relating directly in space and time to the disruptive event, whereas indirect damages are the subsequent losses induced by direct ones, including business interruption losses of affected economic sectors, the spread of losses toward other initially non-affected sectors, and the costs of recovery processes. They often occur, in space or time, after or outside the disaster event.

overproduction capacities as additional flexibilities in the production system, compared to traditional IO models (Halle-gatte, 2014). It has been widely used in single-hazard analysis to simulate the propagation of negative shocks throughout the economy (Guan et al., 2020; Koks et al., 2015; Zhang et al., 2019). Recently, Guan et al. (2020) proposed an extension of the ARIO-Inventory model, which considers the cross-regional substitutability of suppliers to assess the global supply-chain effects of COVID-19 control measures. Here we draw on this study and characterize the pandemic control into different combinations of duration and strictness of global lockdowns. Strictness represents the percentage by which transportation capacity is reduced relative to the pre-pandemic levels. Considering the compound hazards of extreme weather (e.g., flooding), pandemic control, and export restrictions, our impact model made two improvements following this extended ARIO-Inventory model. First, it analyses the interaction between climate and pandemic responses, that is, the negative externality of pandemic control on the recovery of capital destroyed by natural disasters and the stimulus effects of capital reconstruction to offset the negative impacts of pandemic control. Second, it considers the roles of export restrictions and production specialization in exacerbating the economic consequences of compound events. Export restriction is a common trade policy signaling deglobalization, whereas production specialization reduces the substitutability of regional products and may increase the economic vulnerability for negative shocks (Boehm et al., 2019).

Although the impacts of extreme weather events on economic growth can last for many years (Hsiang & Jina, 2014; Lackner, 2018), the compound-hazard impact model proposed here is mainly intended for a short-term analysis, as it is focused on the impacts between the compound shock and the return to the pre-shock economic state in 1 or 2 years (without growth).

It should be noted that when we mention pandemic impact in this study, we do not mean the impact of pandemic itself, but the shock of its control measures, mainly referred to as the lockdowns, to the economy. The total impact (including the health impact) of the pandemic might be huge (Cutler & Summers, 2020), but here we only focus on the economic impact of a global control. The monetarized values of premature deaths and health impairment caused by coronavirus infections are not within our research scope. We recognize that differences exist in many aspects among the pandemic control, flooding, and export restrictions, and it is unrealistic to cover all these differences in our compound-hazard impact model. As the model is mainly aimed for the economic impact assessment, we then only extract features that are of economic relevance and parameterize them with different values (such as different durations, intensities, and spatial spreads) for different events in the model. To keep it simple, we do not distinguish the specific warning, impact, and response phases of different events, rather than considering them as a whole in our scenario settings.

In our modeling, the three types of events enter the economic system in different ways given their different characteristics, but they all cause indirect impact, which sometimes intertwines, through both backward and forward propagations along the supply chain. First, the flood impacts start with the direct damage to labors and capital stock and the increasing reconstruction needs. The labor/capital damage limits the production and supply of the flooded economic sectors, which propagates forward to the production of downstream sectors because of an input shortage. There are also large backward propagations to upstream sectors through reduced demands (when the flooded sectors have lower production capacities) or increased demands (due to reconstruction needs). Second, the pandemic control affects the economy by restricting the transportation capacity and labor availability, which is different from flood impact. However, this is also accompanied by forward and backward propagations due to delivery failures of intermediate inputs and reduced demand at a low production capacity. Meanwhile, the transport restriction also impedes the process of flood-related reconstruction, which exacerbates the indirect impact. Third, a trade restriction limits the maximum export of specific products from a region to another region below a certain percentage of the previous level. It causes both forward propagations (when the importing sectors in the latter region produce less due to a shortage of imported input) and backward propagations (as the exporting sectors in the former region also produce less due to a reduced export demand), which is similar and entangled with flood and pandemic impact. This is how we package the three types of hazards into a macroeconomic risk assessment. Although these events are different in many aspects, they have similar and intertwined risk transmission channels within the economic system.

Figure 1 presents the framework of our impact model, which is driven by four modules, that is, an external shock module, a production module, an allocation module, and a demand module. The external shock module refers to the negative shocks of flooding, pandemic control, and export restriction on various aspects of the economy. The production module describes the sectors' production activities under production, transport, and import capacity constraints. The allocation module explains how sectors allocate output to their clients, including downstream sectors and households, to satisfy the intermediate demand for inventory refilling and final demand for consumption and reconstruction. Finally, the demand module portrays how clients issue orders to their suppliers, which iterates into the next round of production until the economy recovers to the pre-disaster state.

Our compound-hazard impact model starts with a global economy in equilibrium. We define two types of economic agents, namely, sectors and households, distributed in R regions. Sectors make products that can be consumed by either downstream sectors or households. There is a total of P types of products, one-to-one corresponding to P production sectors; therefore, there are up to $R \times P$ sectors in the economy. For simplification purposes, we use a

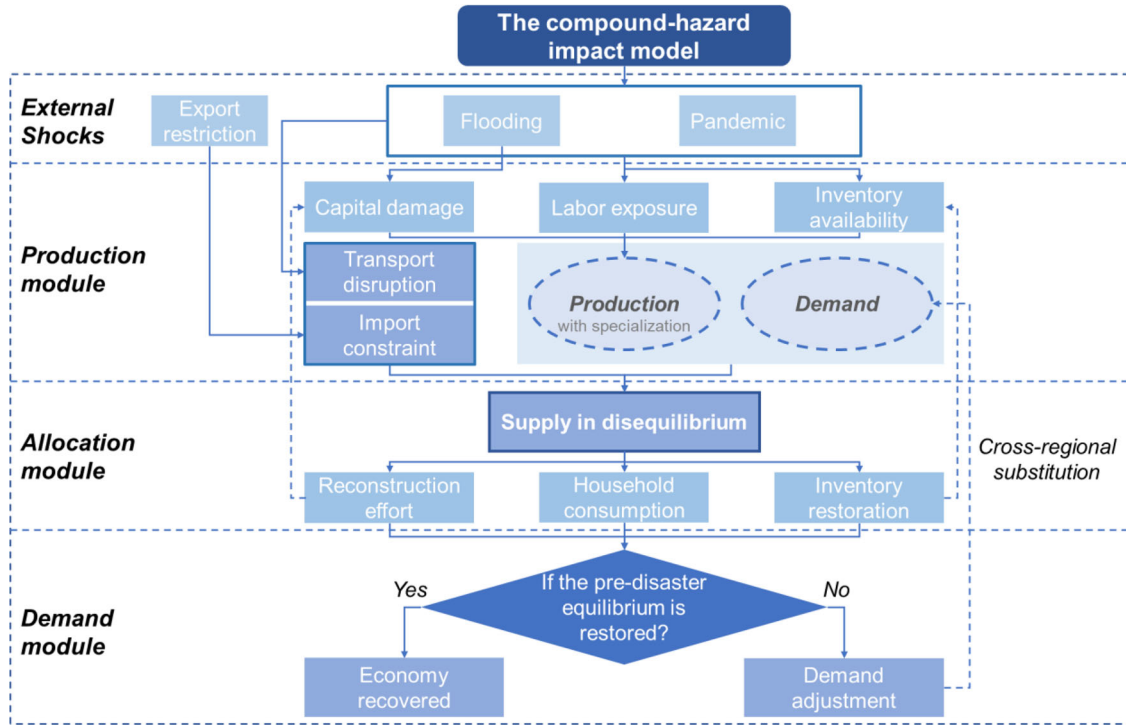


FIGURE 1 Framework of the compound-hazard impact model.

representative household that consumes multiple types of products to represent all the households in a region. The total number of representative households in the economy is equal to R . A brief description of key variables used in the model is listed in Table A.1.

2.1 | Compound exogenous shocks

We mainly focus on four categories of direct shocks introduced by a perfect storm to an economic system, that is, damages to production factors (e.g., capital and labor), transport disruptions, export restrictions, and consumption adaption.

2.1.1 | Capital damage

The amount of productive capital is reduced as physical assets, such as factories, machines, and equipment, are inundated by flooding and out of operation. The damaged capital can also be recovered by post-flood reconstruction activities. The capital stock held by sector i in region r at time t is expressed as

$$K_{ir}(t) = K_{ir}(t-1) - K_{ir}^F(t) + K_{ir}^{REC}(t-1), \quad (1)$$

where $K_{ir}(t)$ is the surviving capital stock of sector i in region r at time t . $K_{ir}^F(t)$ refers to the amount of capital damaged by flooding alone. We assume that the pandemic control has no direct impact on productive capital. $K_{ir}^{REC}(t-1)$ repre-

sents the recovered capital at the end of period $t-1$ (see Equation 15).

We use $\gamma_{ir}^K(t)$ to denote the percentage reduction in the capital stock of sector i in region r at time t , relative to the pre-disaster level, as follows:

$$\gamma_{ir}^K(t) = \frac{\bar{K}_{ir} - K_{ir}(t)}{\bar{K}_{ir}}, \quad (2)$$

where \bar{K}_{ir} is the capital stock held by sector i in region r at the pre-disaster level. In this article, we use overbars to indicate values at the pre-disaster equilibrium levels.

2.1.2 | Shocks to labor, transport, export, and final demand

Labor supply is damaged by both flooding and pandemic crises. First, fewer employees can work because of injury, illness, or death from flooding and virus infection. Second, healthy employees spend more time commuting to and from work due to transport disruptions, which results in working time losses. The shortage or malfunction of production factors will reduce the sectors' production capacity.

Transport disruptions come from two aspects during the perfect storm. First, public transport restrictions are placed in the epidemic regions to contain virus transmission. Second, the transport infrastructure could also be inundated and out of operation when the region is hit by a flood. Transport disruptions not only affect labor supply but also increase the

difficulty in delivering the intermediate and final products to downstream sectors and households.

Countries/regions may impose export restrictions on products to secure domestic supply in the short run following the compound crises. However, this would reduce the import capacity of downstream clients. The importing countries/regions without sufficient production capacity will suffer a shortage of supply of those restricted products (World Trade Organization, 2020).

Households might also adjust their consumption in response to the perfect storm. For example, they may spend less on restaurants, traveling, and other outdoor recreational activities, whereas more on medical services and emergency products. The adaptive behavior of consumers during or after the event will lead to structural changes of the final demands in the short term.

These four categories of direct impacts are not isolated. For example, the unavailability of transportation may lead to labor constraints. Restoring damaged productive capital, as well as export restrictions, will affect the structure of final demands in the disaster aftermath. The interactions between direct shocks lead to complex indirect impacts on the economic system. Therefore, a systematic assessment method is needed to address these issues. A full description about these shocks and their interrelationship is provided in Section A.2.

2.2 | Production system

2.2.1 | Production with cross-regional substitution and specialization

Economic sectors rent capital and employ labor to process natural resources and intermediate inputs produced by other sectors into a specific product. Traditional IO models adopt the Leontief production function where different inputs are used in fixed proportions during production and are not mutually substitutable (Miller & Blair, 2009). This may overestimate the economic losses from negative shocks (Okuyama & Santos, 2014). Later, Guan et al. (2020) improved on this issue by incorporating the possibility of cross-regional substitution in their analysis where products of a sector in a region can be substituted by products of the same sector from a different region. However, some products are less substitutable between regions, particularly when production specialization occurs. For example, Boehm et al. (2019) discovered that during the Japanese earthquake, the economic losses in the United States are highly concentrated among affiliates of Japanese multinationals, relative to non-Japanese firms, due to declines in imported intermediate inputs from Japan. This suggests that affiliates of Japanese firms in the United States were unable to quickly substitute alternative inputs in the short run. Besides, the recent shortage of microchips, which is driven by the perfect storm of multiple factors, such as pandemic outbreaks, a fire in an

automotive chip plant in Japan, the trade friction between the United States and China, has greatly hampered automotive production in the United States (McCarthy, 2021). Most of the microchip production is dominated by two foundries in Asia, namely, TSMC and Samsung, and their customers lack alternative suppliers who can quickly build a new microchip fab or catch up with the leading-edge process technologies (Kuo, 2021).

This study improves on Guan et al. (2020) by incorporating non-substitutable specialized products. Although we keep the possibility of cross-regional substitution, specialized products cannot be substituted elsewhere. There are two types of non-substitutability. The first one is non-substitutability between the P sectors, that is, products of a sector cannot be substituted by products of a different sector, though can be substituted by products of the same sector from a different region. The second one is the non-substitutability of specialized products which is different from and cannot be substituted by any products in any sectors or regions. We assume that there are Q types of specialized products, each one belonging to one of the P production sectors in one of the R regions. Then sectors can use $P + Q$ different types of mutually non-substitutable intermediate inputs to produce their products. The production process is defined as

$$x_{ir} = \min \left\{ \text{for all } j, \frac{z_{j,ir}}{a_{j,ir}}; \quad \text{for all } k, \frac{v_{k,ir}}{b_{k,ir}} \right\},$$

$$j = 1, \dots, P + Q, k = 1, 2, \quad (3)$$

where x_{ir} denotes the output of sector i in region r . $z_{j,ir}$ and $v_{k,ir}$ are the intermediate input j and primary input k (i.e., capital and labor), respectively, used to produce x_{ir} amount of output. $a_{j,ir}$ and $b_{k,ir}$ are the input coefficients indicating the amount of intermediate input j and primary input k required to produce one unit of product i in region r , as follows:

$$a_{j,ir} = \frac{\bar{z}_{j,ir}}{\bar{x}_{ir}} \quad (4)$$

and

$$b_{k,ir} = \frac{\bar{v}_{k,ir}}{\bar{x}_{ir}}, \quad (5)$$

where $\bar{z}_{j,ir}$, $\bar{v}_{k,ir}$, and \bar{x}_{ir} are the intermediate input, primary input, and output of sector i in region r at the pre-disaster levels, respectively.

Equation (3) looks like a Leontief production function but does not distinguish between intermediate products j from different regions, as we allow for substitution between products, if not specialized, of the same sector from different regions. Besides, we add the Q specialized products in Equation (3), as we consider them to be different and non-substitutable from any other input.

2.2.2 | Production under compound constraints

In an equilibrium state, sectors use intermediate and primary inputs to produce goods and services to satisfy demand from their clients. After the perfect storm, output will decrease due to the capital, labor, and inventory constraints.

First, embodied in the essence of IO modeling where capital and labor are considered perfectly complementary and fully employed in the economy, we assume damage in capital assets is linearly related to production level and, therefore, value-added level. Then, the capital productive capacity of sector i in region r at time t , $x_{ir}^K(t)$, is constrained by the proportion of the available capital relative to the pre-disaster level, as follows:

$$x_{ir}^K(t) = \alpha_{ir}(t) \times (1 - \gamma_{ir}^K(t)) \times \bar{x}_{ir}, \quad (6)$$

where $\gamma_{ir}^K(t)$ is the proportion of capital damaged by the perfect storm (Equation 2), and $\alpha_{ir}(t)$ is the overproduction capacity modeled in Equation (23).

Similarly, the labor productive capacity, $x_{ir}^L(t)$, is

$$x_{ir}^L(t) = \alpha_{ir}(t) \times (1 - \gamma_{ir}^L(t)) \times \bar{x}_{ir}, \quad (7)$$

where $\gamma_{ir}^L(t)$ is the proportion of labor damaged by the perfect storm (Equation A.2).

Finally, an insufficient inventory of a sector's intermediate products will create a bottleneck for production activities. The potential production level, $x_{ir}^j(t)$, that the inventory of the intermediate product j can support is

$$x_{ir}^j(t) = \frac{S_{ir}^j(t-1)}{a_{j,ir}}, \quad j = 1, \dots, P + Q, \quad (8)$$

where $S_{ir}^j(t-1)$ refers to the amount of intermediate product j held by sector i in region r at the end of time $t-1$. j is one of the $P + Q$ types of mutually non-substitutable intermediate products mentioned in Section 2.2.1.

Considering all these constraints, the maximum production capacity, $x_{ir}^{\max}(t)$, of sector i in region r is expressed as follows:

$$x_{ir}^{\max}(t) = \min \left\{ x_{ir}^K(t); x_{ir}^L(t); \text{ for all } j, x_{ir}^j(t) \right\}, \quad j = 1, \dots, P + Q. \quad (9)$$

The actual production of sector i in region r depends on both its maximum production capacity and the total orders it expects to receive from its clients:

$$x_{ir}^a(t) = \min \left\{ x_{ir}^{\max}(t), TD_{ir}(t-1) \right\}. \quad (10)$$

Here we assume that the sector always expects to receive the same quantities of orders as the previous period, that is, $TD_{ir}(t-1)$ (Equation 22).

Therefore, the inventory of product j held by sector i in region r will be consumed during the production process. We use $S_{ir}^{j,used}(t)$ to denote the amount of intermediate product j used in the production of this sector at time t , which is

$$S_{ir}^{j,used}(t) = a_{j,ir} \times x_{ir}^a(t). \quad (11)$$

2.3 | Allocation and recovery

Demand in the aftermath of a perfect storm can be categorized into three strands, that is, intermediate demand, final demand, and reconstruction demand. Products made under constraints induced by the compound event will flow to these demands on the market. However, probably not all demands can be met by outputs under constraints, which causes the disequilibrium of the economy. We use a prioritized-proportional rationing scheme that is subject to export restrictions to model the resource allocation process during the disequilibrium period.

2.3.1 | Prioritized-proportional rationing scheme under export restrictions

Under the prioritized-proportional rationing scheme, we assume that a sector first allocates its output to address the intermediate demand and then proportionally allocates the remaining output to other categories of demand. This assumption is based on the observation that business-to-business relationships are stronger than business-to-client relationships and therefore should be prioritized (Hallegatte, 2008; Li et al., 2013). This rationing process is similar to Zeng et al. (2019) except that it is constrained by export restrictions, that is, the total export of a sector at each time step should be no more than its maximum quota restricted by the trade policy:

$$\sum_{s \neq r} \sum_{j=1}^P FRC_{js}^{ir,*}(t) + \sum_{h \neq r} HRC_h^{ir,*}(t) + \sum_{s \neq r} \sum_{j=1}^P RRC_{js}^{ir,*}(t) \leq (1 - \gamma_{ir}^E(t)) \times \bar{e}x_{ir}, \quad (12)$$

where $FRC_{js}^{ir,*}(t)$, $HRC_h^{ir,*}(t)$, and $RRC_{js}^{ir,*}(t)$ are the output of sector i in region r allocated to sector j in region s as intermediate use, to household in region h as consumption use and to sector j in region s as reconstruction use, respectively, as time t under export restrictions. $\gamma_{ir}^E(t)$ is the degree of export restriction imposed on product i by region r at time t . It is measured by the percentage reduction of the maximum export volume of this product in region r relative to the pre-disaster level (see Section 2.1.2 and Section A.2.3). $\bar{e}x_{ir}$ represents the export of this product from region r to other regions under the

pre-disaster equilibrium state. A detailed description about this part is given in Section A.3.

2.3.2 | Recovery of inventory and capital stock

The sector j in region s receives intermediates from all relevant regions to restore its inventories of product i at time step t , as follows:

$$S_{js}^{i,restored}(t) = \sum_{r \in R^i} FRC_{js}^{ir,*}(t), \quad i = 1, \dots, P + Q, \quad (13)$$

where R^i refers to the set of regions that supply product i . If product i is a specialized product of sector i in region r , then r is the only region making product i and $R^i = \{r\}$.

Therefore, the quantities of intermediates i held by sector j in region s at the end of period t are

$$S_{js}^i(t) = S_{js}^i(t-1) - S_{js}^{i,used}(t) + S_{js}^{i,restored}(t). \quad (14)$$

Similarly, the recovered capital of sector j in region s at the end of period t is equal to

$$K_{js}^{REC}(t) = \sum_{r=1}^R \sum_{i=1}^P RRC_{js}^{ir,*}(t). \quad (15)$$

2.4 | Demand adjustment

At the end of each period, downstream sectors and households issue orders to their suppliers according to their production, consumption, and reconstruction plans for the next period. When a product comes from multiple suppliers, the orders are redistributed among suppliers from different regions according to their transport, export, and production capacities.

2.4.1 | Intermediate demand

A sector issues orders to its suppliers because of the need to restore its intermediate product inventory. We assume that sector j in region s has a specific targeted inventory level of product i , $S_{js}^{i,G}$, which is equal to a given number of weeks, n_{js}^i , of intermediate consumption of product i , based on its production capacity at the pre-disaster level:

$$S_{js}^{i,G} = n_{js}^i \times a_{ijs} \times \bar{x}_{js}, \quad i = 1, \dots, P + Q. \quad (16)$$

To fill the gap between the targeted and the actual inventory levels of intermediate product i , the sector j in region s will allocate its orders among suppliers of product i from different regions based on their transport, export, and production capacities. Then the order issued by sector j in region s to its

supplier of sector i in region r is

$$FOD_{js}^{ir}(t) = \begin{cases} \left(S_{js}^{i,G}(t) - S_{js}^i(t) \right) \times \frac{\overline{FOD}_{js}^{ir} \times (1 - \gamma_{ir,js}^Z(t)) \times (1 - \gamma_{ir}^E(t)) \times x_{ir}^a(t)}{\sum_{r \in R^i} \overline{FOD}_{js}^{ir} \times (1 - \gamma_{ir,js}^Z(t)) \times (1 - \gamma_{ir}^E(t)) \times x_{ir}^a(t)}, & \text{if } S_{js}^{i,G}(t) > S_{js}^i(t) \\ 0 & \text{if } S_{js}^{i,G}(t) \leq S_{js}^i(t), \end{cases} \quad (17)$$

where \overline{FOD}_{js}^{ir} refers to the order issued by sector j in region s to its supplier of sector i in region r at the pre-disaster level. $1 - \gamma_{ir,js}^Z(t)$ represents the capacity to transport the product of sector i in region r to sector j in region s at time t (Equation A.5). $1 - \gamma_{ir}^E(t)$ refers to the capacity to export the product of sector i in region r to sector j in region s at time t . If $s = r$, then $\gamma_{ir}^E(t)$ is equal to zero here.

2.4.2 | Final demand

Similarly, households allocate orders among their suppliers from different regions based on their adaptive demand and the transport, export, and production capacities of their suppliers. The total adaptive demand of the household in region h to final product i at time t is obtained by adding up the demand from different regions, as follows:

$$HD_h^i(t) = \sum_{r \in R^i} hd_{ir,h}(t), \quad i = 1, \dots, P + Q, \quad (18)$$

where $hd_{ir,h}(t)$ denotes the adaptive demand of the household h for product i in region r at time t (Equation A.7).

Then, the order issued by household h to its supplier of product i in region r is

$$HOD_h^{ir}(t) = HD_h^i(t) \times \frac{\overline{HOD}_h^{ir} \times (1 - \gamma_{ir,h}^Z(t)) \times (1 - \gamma_{ir}^E(t)) \times x_{ir}^a(t)}{\sum_{r \in R^i} \overline{HOD}_h^{ir} \times (1 - \gamma_{ir,h}^Z(t)) \times (1 - \gamma_{ir}^E(t)) \times x_{ir}^a(t)}, \quad (19)$$

where \overline{HOD}_h^{ir} refers to the order issued by the household h to its supplier of sector i in region r at the pre-disaster level. $1 - \gamma_{ir,h}^Z(t)$ represents the capacity to transport the product of sector i in region r to the household in region h at time t (Equation A.6).

2.4.3 | Reconstruction demand

A sector also issues orders to its suppliers because of the reconstruction demand to recover its damaged capital. Here we follow the assumption in Hallegatte (2008) that capital damage will all be repaired, and that insurance companies will pay the whole repair cost. We also assume that sector j in region s targets its capital stock at the pre-disaster level, \overline{K}_{js} .

We use the capital matrix coefficient, d_{js}^{ir} , to express the quantities of product i in region r invested in one unit of capital formation in sector j in region s . Therefore, the total demand for product i to support reconstruction by sector j in region s at time t , $RD_{js}^i(t)$, is

$$RD_{js}^i(t) = \sum_{r \in R^i} \left(\bar{K}_{js} - K_{js}(t) \right) \times d_{js}^{ir}, \quad i = 1, \dots, P + Q, \quad (20)$$

where $K_{js}(t)$ is the capital stock held by sector j in region s at time t derived from Equation (1).

Then the order issued by sector j in region s to support its reconstruction of damaged capital to the supplier of product i in region r is

$$ROD_{js}^{ir}(t) = RD_{js}^i(t) \times \frac{d_{js}^{ir} \times \left(1 - \gamma_{ir,js}^Z(t) \right) \times \left(1 - \gamma_{ir}^E(t) \right) \times x_{ir}^a(t)}{\sum_{r \in R^i} d_{js}^{ir} \times \left(1 - \gamma_{ir,js}^Z(t) \right) \times \left(1 - \gamma_{ir}^E(t) \right) \times x_{ir}^a(t)}. \quad (21)$$

Finally, the total order received by sector i in region r is

$$TD_{ir}(t) = \sum_{s=1}^R \sum_{j=1}^P FOD_{js}^{ir}(t) + \sum_{h=1}^R HOD_h^{ir}(t) + \sum_{s=1}^R \sum_{j=1}^P ROD_{js}^{ir}(t). \quad (22)$$

2.4.4 | Overproduction capacity

The overproduction capacity is modeled with the variable α_{ir} following similar principles as in Hallegatte (2014):

$$\alpha_{ir}(t+1) = \alpha_{ir}(t) + \frac{\alpha_{ir}^{\max} - \bar{\alpha}_{ir}}{\tau_\alpha} \times \frac{TD_{ir}(t) - x_{ir}^{\max}(t)}{\bar{x}_{ir}}. \quad (23)$$

It assumes that the overproduction capacity α_{ir} can increase up to a maximum value α_{ir}^{\max} in a time delay τ_α in response to production shortages and also goes back to the pre-disaster level $\bar{\alpha}_{ir}$ (equal to one) when the situation becomes normal. The last term $\frac{TD_{ir}(t) - x_{ir}^{\max}(t)}{\bar{x}_{ir}}$ represents the gap between production capacity and total demand, relative to the pre-disaster output level. It determines the direction and size of the movement of α_{ir} at each time step. α_{ir} increases/decreases when the gap is positive/negative, and the size of such movement decreases to zero when the gap is narrowed to zero. This mechanism ensures the convergence of the overproduction capacity over time.

2.5 | Economic footprint of a perfect storm

Following a perfect storm, sectors and households in all regions go through the above production, allocation, recovery, and demand adjustment procedures recursively, until a full economic recovery to the pre-disaster level after all con-

straints are lifted (i.e., damaged productive capital is fully recovered, all labor constraints are lifted, and all business linkages are repaired). We define the value-added decrease of all sectors during this process as the economic footprint/impacts of the perfect storm. The impacts of the initial exogenous shocks continuously propagate through the supply chain, from one sector to another and one region to another, leaving footprint in the economic network. The economic footprint of the perfect storm is calculated as follows:

$$Footprint = \sum_{r=1}^R \sum_{i=1}^P \sum_t \left(\bar{v}a_{ir} - v a_{ir}(t) \right), \quad (24)$$

where $\bar{v}a_{ir}$ and $v a_{ir}(t)$ are the value added of sector i in region r at the pre-disaster level and at time t , respectively. The value added of a sector is equal to the value of output minus the value of intermediate input used to produce that output, as follows:

$$v a_{ir}(t) = x_{ir}^a(t) - \sum_{s=1}^R \sum_{j=1}^P a_{js,ir} \times x_{ir}^a(t), \quad (25)$$

where $a_{js,ir}$ is the input coefficient derived from the IO matrix indicating the input of product j in region s required to produce one unit of product i in region r .

2.6 | Simulation of a hypothetical global economy

We apply our compound-hazard impact model to a hypothetical global economy consisting of four regions and five sectors based on the multi-regional IO (MRIO) table developed by Zheng et al. (2020) (Table B.1).² The annual GDP of this hypothetical global economy is 9613 units. The four regions are denoted by A–D, which account for 21%, 39%, 28%, and 12% of the global economy, respectively. C is the only region hit by flooding, amid a global pandemic control and intensifying trade tensions. B is the largest trade partner of C. More than half (52%) of C's total trade volume comes from region B, which is equivalent to 11% of C's output. This is followed by A and D, which accounts for 31% and 17% of C's total trade volume, respectively. The five sectors include agriculture (AGR), general manufacturing (MANG), capital manufacturing (MANR), construction (CON), and other services (OTH). "MANR" and "CON" are the two sectors

² We adopt this MRIO table because of its open accessibility from the CEADs database (www.ceads.net). It is originally a China multiregional input–output table for 2015, covering 31 provinces and 42 socioeconomic sectors. We aggregate this table into four major regions and five sectors to construct a virtual global economy with almost real and differentiated interregional or inter-sectoral linkages. This helps to enlighten on how different agents in a global network react to compound shocks. We also examine the robustness of our analysis using a different GTAP-based MRIO matrix and find consistent results on the economic interplay among flooding, pandemic control, and trade restrictions (Table B2 and Section C.3.5).

TABLE 1 Parameters of the model

Parameters	Definitions	Values
n_{ir}^j	Weeks of intermediate use of inventory product j that sector i in region r wants to hold	4
α_{ir}^{\max}	Maximum overproduction capacity of sector i in region r relative to the pre-disaster level	125%
τ_α	Weeks needed by a sector to achieve its maximum overproduction capacity	52

TABLE 2 Event settings of flooding and pandemic control

Flooding	Scales	Direct damage ^a (% losses)					Duration (weeks)	Spreads	
		Labor	AGR	MANG	MANR	CON			OTH
	Small (%)	20	20	10	10	15	15	2	Region C
	Medium (%)	40	40	20	20	30	30		
	Large (%)	60	60	30	30	45	45		
Pandemic control	Strictness scenarios (%) (30%, 60% of transportation capacity reduction)						[8, 24]	All regions	

^aDirect damage of flooding refers to the percentage reduction in labor availability and capital stock in the five production sectors: AGR—agriculture; MANG—manufacture, general; MANR—manufacture, capital; CON—construction; OTH—other services.

that are involved in the reconstruction of capital damaged by flooding.

We assume that capital reconstruction largely relies on local inputs of capital goods and construction services, and different sectors in the same region have the same capital matrix coefficients. For example, the “CON” and “MANR” sectors of C contribute to 68% and 20% of the reconstruction efforts in C, respectively, whereas the remaining 12% comes from the “MANR” and “CON” sectors of B and the “MANR” sector of A. A full capital matrix indicating the sources of capital formation of each region is provided in Table B.3.

Values of other parameters in the model are presented in Table 1. Although the values of α_{ir}^{\max} and τ_α are the same as in Hallegatte (2014), the value of n_{ir}^j is smaller than that in Hallegatte (2014). This is due to our assumption of a just-in-time (JIT) inventory management that is gaining popularity for its advantages in lowering inventory and related costs (Yang et al., 2021). In fact, some multinational corporates, such as Hyundai Motor in South Korea, were threatened to suspend production by the supply disruption of inventories around 1 month after the coronavirus outbreak in China (Reuters, 2020). The uncertainty in all these values must be acknowledged, and a sensitivity analysis on these parameters is provided in Section C.3. The model is run on a weekly basis in this analysis.

3 | SCENARIOS AND DISCUSSION

3.1 | Interaction between pandemic control and flooding in the free trade scenarios

We first simulate the economic impacts of multi-scale floods and/or a global pandemic in a free trade world that consists of four regions: A, B, C, and D. Three scales of floods

are defined according to the severity of damages they cause directly to population and economic sectors (Table 2). All floods occur in week 5 and last for 2 weeks in region C. At the same time, a global pandemic happens in all regions, and measures are taken to bring its spread under control. The strictness of the control policy, which is measured by the percentage reduction of the transportation capacity due to lockdown measures relative to the pre-disaster level, is benchmarked at 30% for 24 weeks.

3.1.1 | Economic impacts of flooding, pandemic control, and their collision

We find a two-way interaction between the flooding and pandemic hazards in terms of economic losses, by comparing the flood-only, pandemic-only, and flood + pandemic scenarios. First, the pandemic control aggravates the flood impacts by hampering the post-flood capital reconstruction, under all flood scales. As in Table 3, the recovery of capital stock damaged by multi-scales of flooding in region C is delayed by 8–10 weeks by the coincidence of a benchmarked global pandemic control. The recovery of global GDP is consequently deferred by 3–7 weeks at different flood scales. Compared to the flood-only scenario, the intervention of pandemic control increases the global economic losses by 1040.6–1144.1 units (10.82%–11.90% of global annual GDP) at different flood scales.

Consistent results are observed on the regional scale by comparing the first and third rows of Figure 2, as all regions suffer additional losses from the concurring pandemic control when they are already affected by flooding in C. For region C, which is the only flooded region, the post-flood recovery curves of its GDP (yellow lines) are significantly flattened and delayed by the intervention of pandemic

TABLE 3 Global economic footprint under the flood-only, pandemic-only, and flood + pandemic scenarios without trade restrictions

Scenarios	Direct damage ^a	Indirect losses ^b	Total impacts	Percentage of global annual GDP	Capital recovery weeks ^c	GDP recovery weeks ^c
Pandemic-only	0.0	1242.6	1242.6	12.9	–	42
Small	Flood-only	317.2	50.0	367.2	3.8	41
	Flood + pandemic	317.2	1194.1	1511.2	15.7	49
Medium	Flood-only	634.3	142.1	776.5	8.1	51
	Flood + pandemic	634.3	1221.6	1856.0	19.3	61
Large	Flood-only	951.5	288.9	1240.4	12.9	60
	Flood + pandemic	951.5	1329.5	2281.0	23.7	70

^aThe direct damage refers to the capital damage due to the inundation of physical assets and occurs only in the flooded region C.

^bThe indirect losses are the GDP losses along the global supply chain caused by the compound event. They start from the directly affected regions and spill over to other regions through inter-sectoral and interregional dependencies.

^cFull recovery is achieved when the amount of capital or global GDP in the disaster aftermaths is within $\pm 0.1\%$ of the pre-disaster level.

control.³ This makes the cumulative losses in region C increase by 176.0–268.3 units, which is equivalent to 6.51%–9.92% of its annual GDP at the pre-disaster level, at different flood scales. However, the greatest loss increases are found in region B, which accounts for nearly half (41%–45%) of the global loss increase, followed by region A (22%–24%), under all flood scales. These two regions first experience slight GDP gains (by 0.21%–0.96% for B and 0.07%–0.34% for A) under the flood-only scenarios (Figure 2a–c) but then suffer significant GDP losses (by 11.56%–12.49% for B and 12.00%–12.41% for A) under the flood + pandemic scenarios (Figure 2g–i). Early economic gains come from the stimulus effect of the reconstruction demand to recover the capital damaged by flooding in C. This happens with the possibility of substitution between suppliers, which is also observed by Koks and Thissen (2016). When region C is flooded and unable to meet the increasing demand for reconstruction, clients will choose suppliers in other regions to restore their damaged capital, which stimulates the economic performance there. Among all regions, B benefits most from flooding in C, as it accounts for the biggest part (52%) of C's trade volumes. Such stimulus effect expands with the flood scales. The gain in B's GDP from a small flood in C is 0.21%, which rises to 0.71% from medium flooding and further to 0.96% in large flooding (Figure 2a–c).

Second, flood response may sometimes alleviate some of the negative impacts of pandemic control due to the stimulus effect of post-flood reconstruction. It only exacerbates the negative pandemic impacts when the flood damage is large enough to exceed such stimulus effect. On the global scale (Table 3), the concurrence of a small or medium flood in region C reduces the supply-chain/indirect losses by 48.6 or 21.0 units, respectively, when the global economy is already burdened by the pandemic. The reduction of losses comes from the stimulus effect of post-flood reconstruction as mentioned above. However, large flood leads to large direct damage and widespread supply chain losses, which surpass the stimulus effect of reconstruction activities and therefore increases the global pandemic impacts by 86.9 units.

On the regional scale, the flood-related alleviation effects of negative pandemic impacts are mainly found in the three non-flooded regions (i.e., A, B, and D), comparing the second and third rows of Figure 2. Taking region B, which benefits most from the stimulus effect of post-flood reconstruction, as an example, its relative GDP losses fall from 12.87% (pandemic-only) to 12.49% (small flood + pandemic), then to

³ Taking the small flood as an example, delays in the recovery of region C could be seen from both Table 2 and Figure 2. In Table 2, capital recovery only takes place in region C, which is hit by the flood. It takes 49 weeks during the compound crises of a small flood and pandemic control, which is 8 weeks more than in the flood-only scenario. In Figure 2, the yellow lines depict the dynamics of GDP recovery in region C by weeks. Comparing with the yellow line in Figure 2a (flood-only), the yellow line in Figure 2g (pandemic + flood) is flattened by the intervention of the pandemic control. It takes about 38 weeks for region C to recover its GDP to the pre-disaster level in Figure 2g, which is around 12 weeks more than in Figure 2a. In addition, the yellow line in Figure 2g is similar with that in Figure 2d (pandemic-only), which is because that the flood impact is so small that the pandemic control has dominated the GDP recovery of region C.

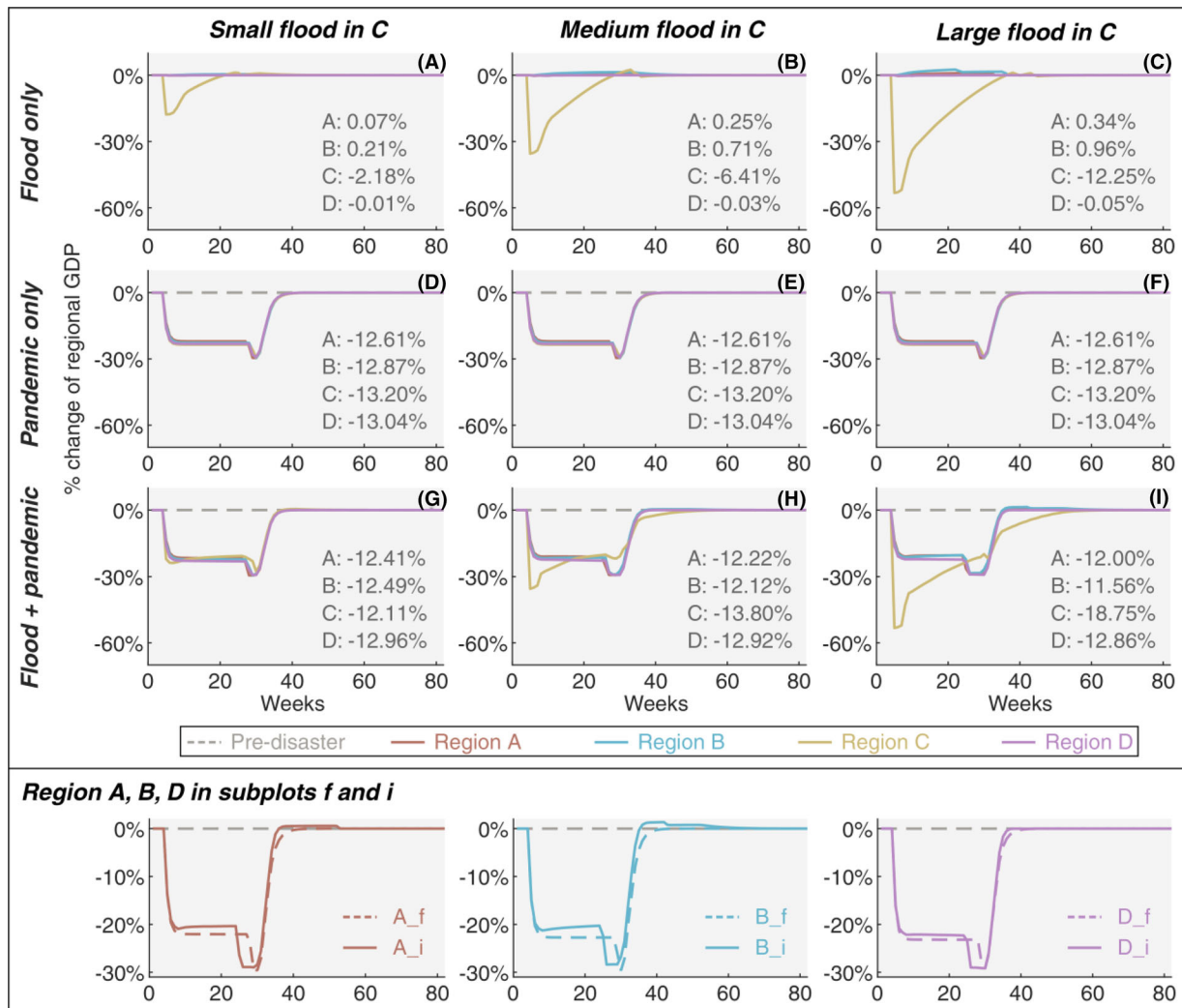


FIGURE 2 Weekly changes of regional GDPs, relative to the pre-disaster levels, in the four regions, under flood-only, pandemic-only, flood + pandemic scenarios without trade restrictions. The numbers in each plot indicate the cumulative losses or gains of regional GDPs over time, relative to the pre-disaster levels of the annual regional GDPs. From left to right, each column represents the small-, medium-, and large-scale flooding in region C. From top to bottom, each row stands for one of the three disaster scenarios: (a) flood-only; (b) pandemic-only; (c) flood + pandemic. The attached row below zooms in on the GDP dynamics of regions A, B, and D in subplots f and i.

12.12% (medium flood + pandemic), and finally to 11.56% (large flood + pandemic). The alleviation effect becomes more significant as the pandemic control intersects with a larger flood. At the bottom of Figure 2, we zoom in on the GDP dynamics of regions A, B, and D in subplots f and i to take a close look at the regional differences between the pandemic-only and large flood + pandemic scenarios. On the one hand, the post-flood reconstruction demand has buffered the negative impact of the pandemic control in the first place for all the three regions and accelerated the GDP recovery of at least region B afterward, which is because that region B is the most involved in region C's capital reconstruction. On the other hand, however, the intervention of flooding also makes the three regions go through earlier and longer shortages of intermediate inputs, which is signaled by further drops of GDPs between weeks 24 and 30, as the pandemic-related transport constraint continues.

By contrast, flood damage aggravates the pandemic impacts in the flooded region C when the flood is above and equal to the medium scale. The region suffers GDP losses of 13.20% from the pandemic control alone, whereas 13.80% from the combination with a medium flood and 18.75% with a large flood. These regional results are in consistency with the global results in revealing the role of the stimulus effect associated with post-flood reconstruction.

In addition, it is worth noting that the continued pandemic control may have a secondary negative impact on regional GDPs by restricting the transport and delivery of intermediate inputs needed to recover production. For example, the second drops of regional GDPs around weeks 28–29 in Figure 2d–f are due to the shortage of intermediate inputs arising from delivery failures under persistent transport constraints during the pandemic control. As mentioned above, the inventory shortage may appear earlier due to the intervention of

flooding and last longer as the flood scale increases (Figure 2g–i). On the contrary, it could be avoided by a shorter but stronger pandemic control (Figure 3g,h). Its occurrence is also linked with the size of inventories held by economic sectors. A large inventory size could improve the inventory resilience and reduce the risk of inventory shortage. As in Section C.3.1 and Figure C.3, the second GDP decline resulting from an inventory shortage in each region is delayed by weeks as the inventory size increases and finally disappears as the inventory size is large enough.

3.1.2 | Pandemic control in different flood periods with different strictness and duration

To investigate how the timing, duration, and strictness of pandemic control impact the economic footprint of the perfect storm, we build three scenario sets: (1) a 30%–24 global pandemic control occurs 7 weeks before flooding; (2) a 30%–24 global pandemic control occurs 7 weeks after flooding; (3) a 60%–8 global pandemic control occurs 7 weeks after flooding. Here the flood hits region C in week 10 and lasts for 2 weeks on the small, medium, or large scale (Table 2). The pandemic control is implemented in all regions.

We summarize the global and regional indirect impacts under these perfect storm scenarios in Table 4 and Figure 3, respectively. Note that we focus on the indirect or GDP losses rather than the direct damage brought by the perfect storm, as the latter is simply correlated with the scale of flooding. First, it is evident from Table 4 that slightly more economic losses are expected when the pandemic control occurs after than before flooding, regardless of the flood scales. The relative losses of global GDP increase by 0.53% (small flood), 0.51% (medium flood), and 0.31% (large flood) when a 30%–24 global pandemic control occurs after than before flooding. On the regional scale, region C suffers the greatest increase in relative GDP losses from the postponement of the pandemic control. For example, the cumulative indirect losses of region C are 19.60% of its annual GDP at the pre-disaster level when a 30%–24 pandemic control takes place 7 weeks before a large flood striking region C (Figure 3c). This figure rises to 20.22% when the control occurs after flooding (Figure 3f). The loss increase of region C is therefore calculated at 0.62%, which is significantly larger than that of region A (0.25%), region B (0.16%), and region D (0.16%). As in Figure 3f, the post-flood economic recovery in region C (the yellow line) is curbed by the pandemic control from week 17, suggesting that a subsequent pandemic control has long-lasting impacts on flood-induced reconstruction and recovery activities.

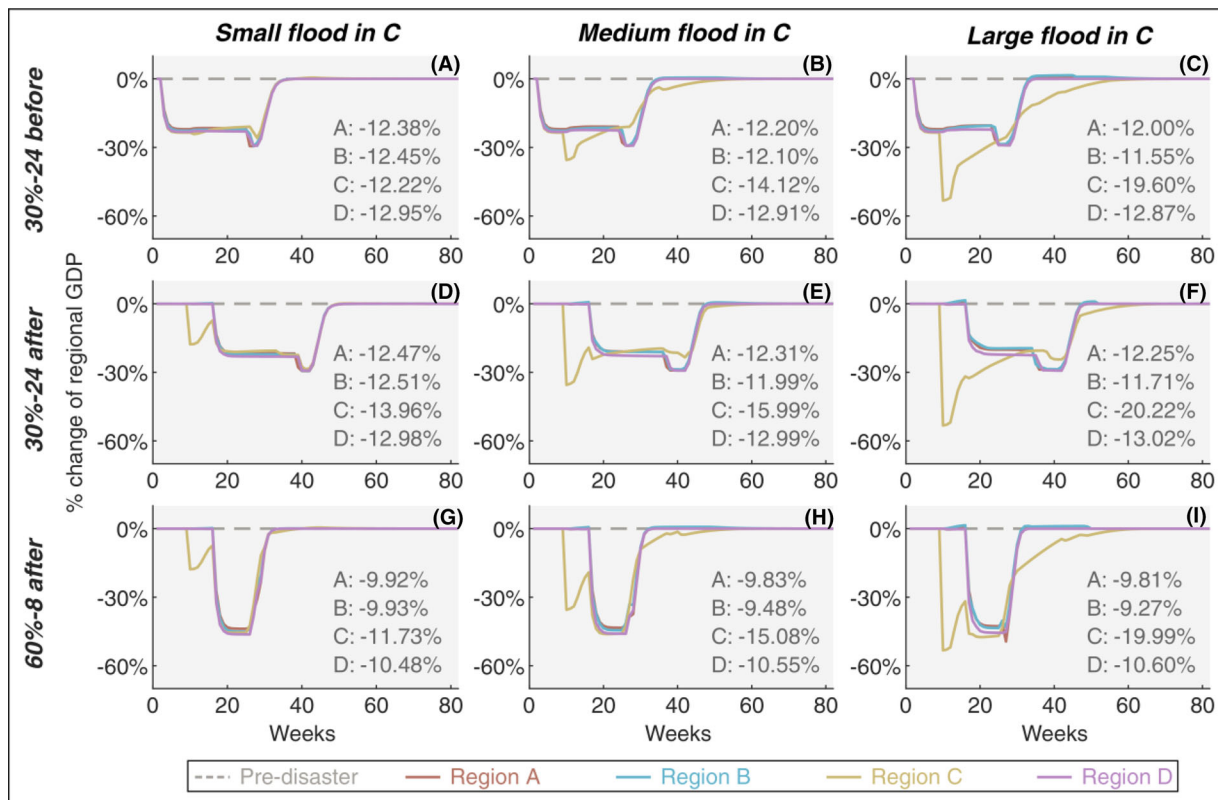


FIGURE 3 Weekly changes of regional GDPs, relative to the pre-disaster levels, in the four regions, when the pandemic control coincides with different flood periods with different strictness and duration. The numbers in each plot indicate the cumulative losses or gains of regional GDPs over time, relative to the pre-disaster levels of the annual regional GDPs. From left to right, each column represents the small-, medium-, and large-scale flooding in region C. From top to bottom, each row stands for one of the three perfect storm scenarios: (a) a 30%–24 global pandemic control takes effect 7 weeks before flooding; (b) a 30%–24 global pandemic control takes effect 7 weeks after flooding; (c) a 60%–8 global pandemic control takes effect 7 weeks after flooding.

TABLE 4 Global indirect impacts, relative to the global annual GDP at the pre-disaster level, of the pandemic control intersecting in different flood periods with different strictness and duration

Scenarios		Flood scales in region C		
		Small (%)	Medium (%)	Large (%)
Global pandemic control	30%–24 control 7 weeks before flooding	12.43	12.79	14.06
	30%–24 control 7 weeks after flooding	12.96	13.30	14.37
	60%–8 control 7 weeks after Flooding	10.50	11.26	12.55

Second, we find that a combination of shorter duration and higher strictness of pandemic control would result in less economic losses for all regions, regardless of the flood scales. As shown in Table 4, the relative losses of global GDP are 14.37% when a 30%–24 pandemic control interfaces with the recovery from a large flood. This figure falls to 12.55% when the strictness–duration combination of the control becomes 60%–8. Similar results are found for the small and medium flood scenarios. The reduction in indirect losses happens ubiquitously in all regions (Figure 3g–i). This is consistent with the results of Guan et al. (2020) who studied the global economic costs of COVID-19 control measures in a single-hazard setting. Therefore, an important insight here is that a stricter pandemic control policy for a shorter duration could reduce economic costs when battling both flooding and a pandemic.

3.2 | Influence of export restrictions on the magnitude of economic losses from the perfect storm

In this section, we explore the scenarios of triple shocks from flooding, pandemic, and export restrictions. Global shocks such as the pandemic increase pressures toward deglobalization, including the imposition of export restrictions on critical goods, such as medical products and food (Eaton, 2021; Espitia et al., 2020). Export restrictions in one region may push other regions to introduce retaliatory restrictions and trigger a domino effect (World Trade Organization, 2020). The importing regions will suffer if they cannot quickly find alternative trading partners, which relates to the substitutability of the restricted products.

We compare two groups of scenarios with different cross-regional substitutabilities of economic production. First, in Section 3.2.1, we assume an ideal situation without production specialization, that is, all products can be replaced by products of the same sector from other regions. We also assume that region C, which suffers from the flood, restricts the export of capital manufacturing products (“MANR-C”) to “protect” its domestic recovery. The export restriction is applied in parallel with the 30%–24 global pandemic control, which coincides with multi-scales of flooding defined in Table 2. The degree of the export restriction, which limits the maximum export volume of the products concerned, is set at 50%. We also explore the impact of different degrees of export restriction in Section C.2. Then we assume that

2 weeks later, other regions, such as region B, take retaliatory restrictions of the same degree on capital manufacturing products (“MANR-B”). We compare the indirect economic impacts under the restrictive trade scenarios with the free trade scenario to analyze the role of trade restrictions in disaster recovery under this ideal situation without production specialization. It is worth mentioning that we focus on these two “MANR” sectors as they produce tradable capital products and face increasing demand during the post-flood reconstruction.

Then in Section 3.2.2, we investigate how production specialization, which creates non-substitutable products, influences the economic footprint of the perfect storm together with trade restrictions. We assume that the “MANR-C” and “MANR-B” sectors make specialized capital products that cannot be substituted elsewhere. We compare the economic consequences under the same restrictive trade scenarios as in Section 3.2.1 with the free trade scenario to study how production specialization interacts with trade restrictions during the compound crises. The settings of trade scenarios with or without production specialization are summarized in Table 5.

3.2.1 | Export restrictions without production specialization

As shown in Table 6 and the first two rows of Figure 4, a 50% export restriction on “MANR-C” raises the global indirect losses by 0.16%–0.23% during different flood and pandemic intersections. The indirect losses in regions A and D increase by an average of 0.43% and 0.45%, respectively, faster than other regions from C’s restrictive trade policy. By comparison, region B experiences a less significant loss increase of around 0.17%. It appears that the export restriction on a specific product has moderate impacts on the importing regions when they can easily find a replacement from other exporters.

As for region C itself, it benefits from the export restriction on “MANR-C” only when the flood is at least the medium scale. On the plus side, the export restriction on “MANR-C” could prevent outflows of capital products and accelerate domestic reconstruction during the flood aftermaths. On the minus side, it may reduce foreign demand for C’s products as other regions import and produce less than before. During the small flood, the demand for capital reconstruction is not enough to compensate for the reduction in foreign demand and hence higher indirect loss in region C from the export restriction (Figure 4a,d). By contrast, a larger flood evokes

TABLE 5 Settings of trade scenarios

Trade scenarios	Definitions	Duration	Production specialization
Free trade	No export restrictions	–	MANR-C and MANR-B if production specialization exists
Restrictive trade without retaliation	50% reduction of the maximum export volume on MANR-C	24 weeks	
Restrictive trade with retaliation	Same degree ^a of retaliatory restrictions from MANR-B 2 weeks after the MANR-C restriction	24 weeks for MANR-C; 22 weeks for MANR-B	

^aDegree of export restriction refers to the percentage reduction of the maximum export volume relative to the pre-disaster level.

TABLE 6 Global indirect impacts, relative to the pre-disaster level of the annual global GDP, of the perfect storm under different trade scenarios without production specialization

Scenarios	30%–24 pandemic control		
	Small flood (%)	Medium flood (%)	Large flood (%)
Free trade	12.42	12.71	13.83
50% Export restriction	On MANR-C	12.65	12.91
	On MANR-C with retaliation from MANR-B	14.34	14.21

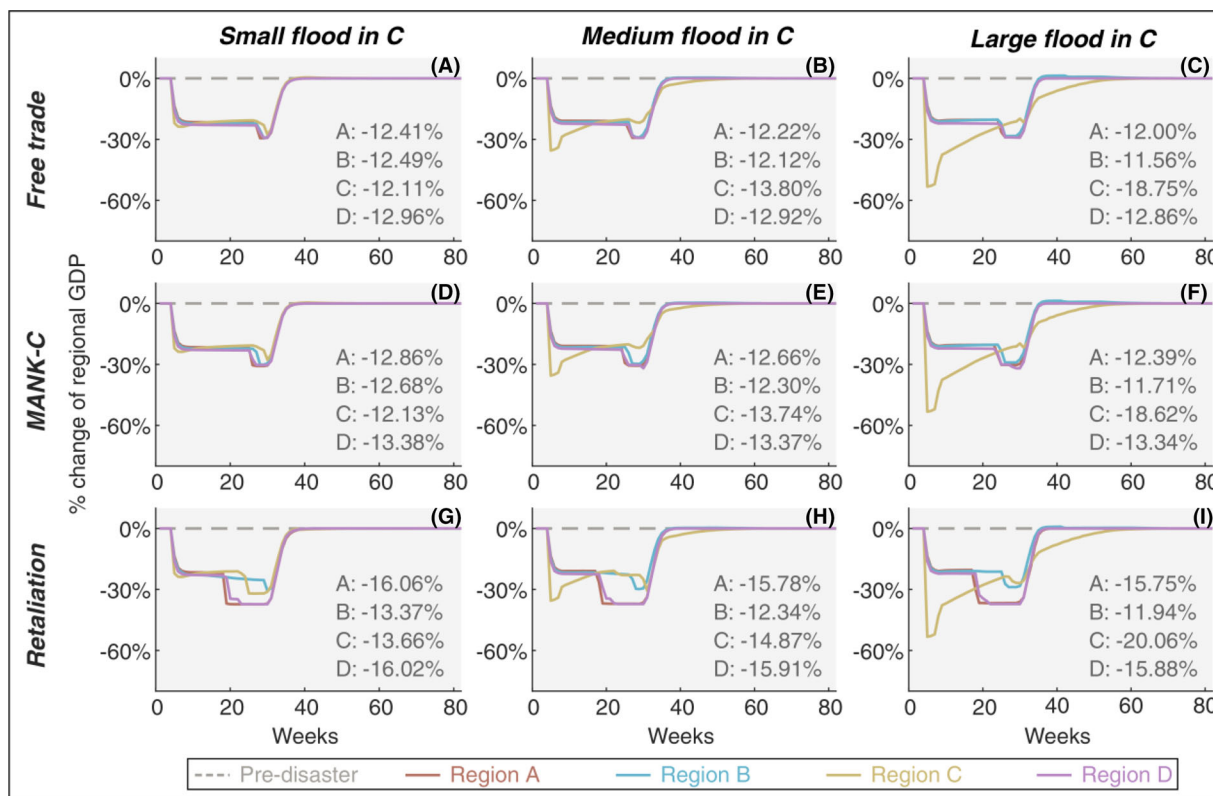


FIGURE 4 Weekly changes of regional GDPs, relative to the pre-disaster levels, in the four regions, when multi-scale floods collide with pandemic control and export restriction without production specialization. The numbers in each plot indicate the cumulative losses or gains of regional GDPs over time, relative to the pre-disaster levels of the annual regional GDPs. From left to right, each column represents the small-, medium-, and large-scale flooding in region C. From top to bottom, each row stands for one of the three export restriction scenarios: (a) free trade scenario without any export restrictions; (b) 50% export restriction on product MANR-C; (c) 50% export restriction on product MANR-C and 2 weeks later 50% retaliatory export restriction on product MANR-B.

higher demand for capital reconstruction, which makes the positive impact of the export restriction outweigh the negative one, that is, the backfire effect of restricting the production of other regions. For example, the indirect loss in region C decreases from 18.75% to 18.62% when region C adopts the export restriction during the confluence of the large flood and pandemic control (Figure 4c,f).

We then consider the impact of a 50% retaliatory export restriction from region B on its “MANR” sector. As shown in Table 6 and the bottom two rows of Figure 4, such retaliation adds another 1.30%–1.69% to the global indirect losses compared to the single “MANR-C” restriction. At the regional level, regions A and D are still the most vulnerable to the escalating trade friction, the cumulative GDP losses of which increase by an average of 3.22% and 2.57%, respectively, during different flood and pandemic intersections. They also encounter inventory shortages earlier than other regions and themselves in the former two trade scenarios. By comparison, region B is the least affected by its trade policy but still goes through an increase by around 0.32% in its indirect losses. This may be partly related to the different levels of trade dependence of the regional economies. Specifically, for regions A and D, their trades with other regions account for around 30% and 31% of their total output, respectively, which are higher than the other two regions. Higher dependence on interregional trade increases economic vulnerability when countries impose trade restrictions.

It is worth noting that region C also suffers increasing indirect losses (by around 1.37%) under all flood scales with retaliation from “MANR-B.” This suggests that it is unwise for region C to initiate trade restrictions in the first place if retaliation is expected in responding to the perfect storm.

Whether at the global or regional level, the indirect losses increase faster with the “MANR-B” restriction than the “MANR-C” restriction, as the former sector is a key node sector in terms of having large trade volumes with other sectors in the economic network. The trade volume with the “MANR-B” sector reaches 8.2% of the global GDP, ranking the third among all sectors, whereas that with the “MANR-C” sector is only 2.7%.

We also investigate how the economic impacts change with the degree of export restriction on “MANR-C” in Section C.2. The results show that both global and regional indirect losses, except for losses of region C, increase with the degree of export restriction. The indirect losses in region C increase with the degree of export restriction when the flood is at the small scale and decrease with the degree of export restriction when the flood is at the medium or large scale. The results found in this section are robust with the degree variations of the export restriction.

3.2.2 | Export restrictions with production specialization

Assuming the “MANR-C” and “MANR-B” sectors make specialized capital products that cannot be substituted else-

where, Table 7 shows that the 50% restriction on the export of “MANR-C” increases global indirect losses by 12.10%–12.73% during the confluence of different scales of floods and the 30%–24 pandemic control, and the accompanying retaliatory restriction on the export of “MANR-B” raises the global indirect losses by another 3.44%–4.09%.

When looking into the regional details, Figure 5 shows that the indirect losses in regions A, B, and D more than double under the compound scenarios with the export restriction on the non-substitutable “MANR-C” as these regions cannot find an alternative to refill the inventory shortage. Specifically, their losses are significantly increased by an average of 16.72%, 16.65%, and 15.97%, respectively, of their annual GDPs. This also in turn damages the post-disaster economic performance of region C, by an additional ~1.72% of its annual GDP, through the propagation effect of the global supply chain. Second, the subsequent retaliation from “MANR-B” has little extra impact on regions A, B, and D, as their production has been already greatly constrained by the inadequate input of “MANR-C”. Instead, region C, which encounters ~13.12% increase in the indirect losses, is severely afflicted by the “MANR-B” retaliation.

Comparing the results in Sections 3.2.1 and 3.2.2, we find that production specialization severely aggravates the economic impact of export restrictions when they collide with each other. In general, the export restriction of a region in response to the compound shock always comes at the cost of global economic resilience, while not necessarily promoting its own recovery, notably with insufficient domestic demand, retaliatory actions, and production specialization. Only when the increase in domestic demand suffices to offset the negative impact of the deterioration of the external economic environment could the region benefit from its restrictive trade policy.

In addition, comparing the two free trade scenarios with or without production specialization in Tables 6 and 7, we find that the production specialization of “MANR-C” and “MANR-B” slightly increases the global losses by 0.01% and 0.46%, respectively, during the medium and large floods colliding with the pandemic control. This indicates that the production specialization, which reduces the cross-regional substitutability of the products concerned, may lead to higher vulnerability of the global economy toward the perfect storm.

Similar to Section 3.2.1, we also examine the sensitivities of the economic impacts to the degree of the export restriction on “MANR-C” with production specialization and find robust results that both global and regional indirect losses (including losses in region C) increase with the degree of the export restriction at faster rates than without production specialization (see Section C.2).

4 | CONCLUSION

In this study, we construct a compound-hazard impact model to simulate the economic footprint of a pandemic-induced perfect storm, taking the collision of flooding,

TABLE 7 Global indirect impacts, relative to the pre-disaster level of the annual global GDP, of the perfect storm under different trade scenarios with production specialization

Scenarios		30%–24 pandemic control		
Scenarios		Small flood (%)	Medium flood (%)	Large flood (%)
Free trade		12.42	12.72	14.29
50% Export restriction	On MANR-C	24.52	25.06	27.02
	On MANR-C with retaliation from MANR-B	28.61	29.03	30.46

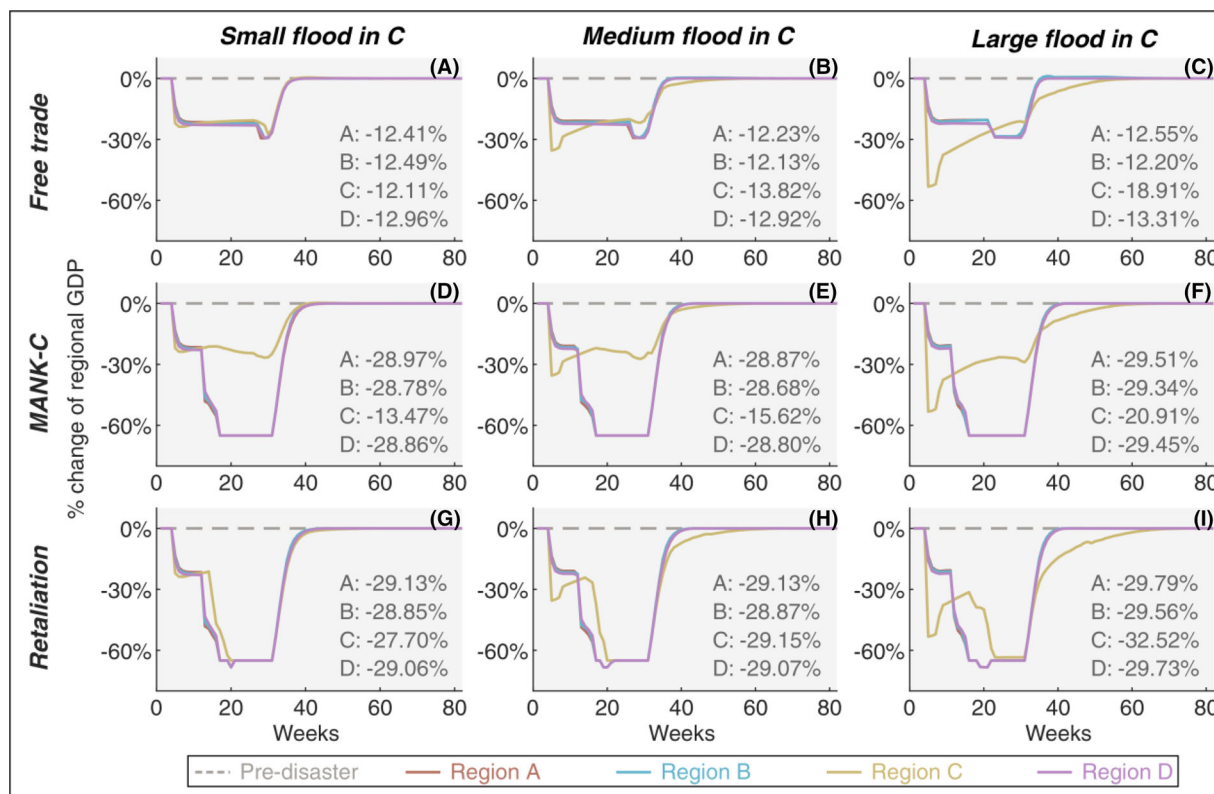


FIGURE 5 Weekly changes of regional GDPs, relative to the pre-disaster levels, in the four regions, when multi-scale floods collide with pandemic control and export restriction with production specialization. The numbers in each plot indicate the cumulative losses or gains of regional GDPs over time, relative to the pre-disaster levels of the annual regional GDPs. From left to right, each column represents the small-, medium-, and large-scale flooding in region C. From top to bottom, each row stands for one of the three export restriction scenarios: (a) free trade scenario without any export restrictions; (b) 50% export restriction on product MANR-C; (c) 50% export restriction on product MANR-C and 2 weeks later 50% retaliatory export restriction on product MANR-B.

pandemic control, and export restrictions as an example. Our compound-hazard impact model improves the standard ARIO model, which is commonly used in single-hazard impact analysis, by considering the interplay between different types of hazardous events for the first time. We also incorporate the possibilities of cross-regional substitution and production specialization, which have opposite impacts on the substitutability of suppliers of the same sector from different regions; thus, the economic resilience toward a perfect storm and estimates of the economic consequences. We build various scenario sets to test the robustness of our model on a hypothetical global economy of four regions and five sectors. These scenarios are designed to investigate how the economic

impacts of the perfect storm react to (1) the timing, strictness, and duration of the pandemic control; (2) the export restrictions imposed on specific sectors and regions; and (3) the presence of specialized production. The latter two special scenario sets are included here as a reflection on the ongoing deglobalization and intensifying trade tensions.

Two major conclusions can be drawn from the simulation results. The first conclusion is about the economic interplay between pandemic control and flood responses in a free trade global economy. On the one hand, a global pandemic control aggravates the flood impacts by hampering the post-flood capital reconstruction. This confirms the idea from an economic perspective that restrictions targeted at coronavirus

containment result in inadequate flood responses, aggravating the flood impacts (Ishiwatari et al., 2020; Selby & Kagawa, 2020; Swaisgood, 2020). On the other hand, a flood disaster exacerbates the pandemic impacts only when the flood damage is large enough to exceed the stimulus effect from the flood-related reconstruction activities. The flood disaster would accelerate and extend the shortage of inventories brought by the pandemic control and increase the negative impact on GDP. Its related reconstruction demand, however, could stimulate regional recoveries, which is also confirmed by Koks and Thissen (2016), and alleviate to some extent the negative impact of the pandemic control.

We make two suggestions on pandemic intervention with flood disasters under the free trade scenarios. First, we suggest an early pandemic intervention strategy to reduce the economic footprint when the pandemic outbreak is colliding with flood disasters. Our results show that when the pandemic control takes place after flooding, this leads to more severe economic impacts than when the control is implemented before the flooding, due to long-lasting disruption of the post-flood recovery. Second, we suggest a stricter but shorter pandemic control to reduce the economic impacts of the perfect storm. We compare the impacts of a 30%–24 pandemic control with a 60%–8 pandemic control applied intermittently in the recovery period of multiple scales of flooding and discover that the latter one results in less economic losses in all regions. This is in-line with one of the major insights provided by Guan et al. (2020).

The second conclusion refers to the role of trade in the economic footprint of compound risks. When the increasing trade barriers intertwine with the collision of flooding and pandemic control, it creates a triangled perfect storm. In general, a region implementing export restriction is always at the cost of global economic recovery, whether it benefits from this policy or not. Although the export restriction prioritizes domestic needs for post-disaster recovery, it does not necessarily mitigate the economic losses of the region if the stimulus of the surge in domestic demand cannot overtake the negative impact of the decline in exports. For other regions, those with high trade dependence would be more vulnerable to the export restriction and suffer faster increases in indirect losses.

For another, specialization, which leads to the concentration of key sectors in particular regions and limits the possibilities for substitution, may sometimes delay economic recovery and raise the vulnerability of the economic network to such compound risks. The export restriction imposed on the non-substitutable specialized sector in a region would put other regions at higher risks with significant surges in economic losses. This may also backfire on the economic resilience of the region itself through the propagation effect of the global supply chain.

A trade restriction may also push other regions to make retaliatory movements, which further deteriorate the global recovery and make everyone lose. Among all the regions, the region which initiates the trade war loses much more when the retaliatory restriction is also imposed on a non-

substitutable product. The collision of export restriction and production specialization, particularly with the expectation of retaliation, can trigger devastating impacts on the global economy at a time when it is already heavily burdened by tackling the compound hazards of extreme weather events and pandemic control.

Therefore, we advocate regional or global cooperation to ease the negative impacts of deglobalization, at least rigorous trade policies that avoid highly specialized sectors are required confronting a perfect storm. Policies that lead to higher trade barriers undermine the efforts of other countries battling extreme weather events and a pandemic. The use of trade restrictions has a particularly deleterious impact in a world with production specialization in key sectors raising the need for effective discipline at the global level of the use of such measures.

Beyond these policy implications, our impact model has demonstrated its flexibility in addressing various compound-hazard scenarios and can help governments refine their emergency policies by identifying the potential positive or negative externalities on wider economic systems. This could be used to guide regional or global cooperation in mitigating such spillover effects of the compound shocks, particularly in the context of deglobalization. Our research also highlights the importance of an integrated approach in managing the compound risks. By utilizing our impact model, people can grasp a better view of the economic interlinkages between multiple hazards that ultimately develop into a perfect storm. Knowing the constraints from one hazard while responding to another assists in the formation of a balanced strategy, which can minimize the economic losses from the trade-offs between emergency response and pandemic control.

Finally, our model provides consistent and comparable loss metrics with that of single-hazard analysis, as it is based on the popular ARIO model in this field. One of the commonly used metrics should be the ratio between indirect and direct economic impacts resulting from a disaster, the so-called cascading effect indicating the resilience of the supply chain toward the disruption (Mendoza-Tinoco et al., 2020). In our analysis, the indirect/direct ratio is 0.16–0.30 for the flood of multiple scales. This is close to the estimate (0.17) of Hallegatte (2014) for Hurricane Katrina, but lower than that (0.39) of Hallegatte (2008) for the same event. This is because our analysis and Hallegatte (2014) both consider a certain level of substitutability and inventory dynamics that improves the economic resilience. Under the compound scenarios, this ratio soars up to 1.27–3.93 with the intervention of pandemic control, further to 1.41–4.35 with export restrictions on substitutable products, and ultimately to 2.73–8.67 when the restrictions are imposed on specialized non-substitutable products. Our model will facilitate future comparisons between various compounds or single hazards under a similar methodological framework.

Nevertheless, our model is limited by not considering technical progress and is relevant for a short-term time scale, where the production patterns of economic sectors do not shift significantly. This outlook explains why we only

consider the substitution between intermediate inputs of the same kind from different regions, rather than the substitution between different types of inputs. Our model follows the assumption in Hallegatte (2008) that capital damage will all be repaired, and that the insurance companies will pay the whole repair cost. The financial constraints for the reconstruction of uninsured capital damage should be considered in future research. In addition, the event settings for flooding, pandemic control, and export restriction in each scenario are simple abstractions of reality, which only characterize their economic-wise features. We do not distinguish their differences in other aspects in the warning, impact, and response phases but focus on their interconnections in economic risk transmission. Admittedly, there are other kinds of interactions between natural and biological hazards, but it is not in our scope to model all these factors. For one thing, some response measures toward flooding, such as evacuation and displacement, could increase the number of people exposed to the pandemic and the burden on the healthcare system. For another, some pandemic mitigation measures like testing, therapeutics, and vaccines may benefit the economic recovery under complex situations. The health-related interactions and the accompanying economic consequences could be incorporated into future studies.

ACKNOWLEDGMENTS

The authors appreciate the time and effort of the editors and reviewers in providing constructive comments that helped to improve the manuscript. This research is supported by the National Natural Science Foundation of China (72091514, 7224100119, and 7221101088), Shenzhen Science and Technology Program (ZDSYS20210623092007023 and JCYJ20200109141218676), and National Key R&D Program of China (2019YFC0810705).

DATA AVAILABILITY STATEMENT

The simulation code and test data can be accessed at <https://github.com/YCathyHu/compound-hazard-economic-footprint-model>.

ORCID

Yixin Hu  <https://orcid.org/0000-0002-3986-9059>

Daoping Wang  <https://orcid.org/0000-0001-5221-4965>

Jingwen Huo  <https://orcid.org/0000-0003-3082-8370>

Lili Yang  <https://orcid.org/0000-0002-7070-9723>

Dabo Guan  <https://orcid.org/0000-0003-3773-3403>

REFERENCES

- AghaKouchak, A., Chiang, F., Huning, L. S., Love, C. A., Mallakpour, I., Mazdiyasi, O., Moftakhari, H. R., Papalexio, S. M., Ragno, E., & Sadegh, M. (2020). Climate extremes and compound hazards in a warming world. *Annual Review of Earth and Planetary Sciences*, 48(1), 519–548. <https://doi.org/10.1146/annurev-earth-071719-055228>
- Aguiar, A., Chepeliev, M., Corong, E. L., McDougall, R., & van der Mensbrugge, D. (2019). The GTAP data base: Version 10. *Journal of Global Economic Analysis*, 4(1), 1–27. <https://doi.org/10.21642/JGEA.040101AF>
- BBC News. (2021). Saharan dust: Orange skies and sandy snow in southern Europe. Retrieved from <https://www.bbc.com/news/av/world-europe-55966867>
- Boehm, C. E., Flaaen, A., & Pandalai-Nayar, N. (2019). Input linkages and the transmission of shocks: Firm-Level evidence from the 2011 Tōhoku earthquake. *The Review of Economics and Statistics*, 101(1), 60–75. https://doi.org/10.1162/rest_a_00750
- Botzen, W. J. W., Deschenes, O., & Sanders, M. (2019). The economic impacts of natural disasters: A review of models and empirical studies. *Review of Environmental Economics and Policy*, 13(2), 167–188. <https://doi.org/10.1093/reep/rez004>
- Boyle, L. (2020). 2020 has been a bleak year in the climate crisis. So here's the good news. Retrieved from <https://www.independent.co.uk/environment/climate-change/climate-change-2020-record-good-news-b1780393.html>
- Bubeck, P., Otto, A., & Weichselgartner, J. (2017). Societal impacts of flood hazards. Oxford Research Encyclopedia of Natural Hazard Science. Retrieved from <https://oxfordre.com/naturalhazardscience/view/10.1093/acrefore/9780199389407.001.0001/acrefore-9780199389407-e-281>
- Chondol, T., Bhardwaj, S., Panda, A. K., & Gupta, A. K. (2020). Multi-hazard risk management during pandemic. In *Integrated risk of pandemic: Covid-19 impacts, resilience and recommendations* (pp. 445–461). Springer Singapore.
- Cutler, D. M., & Summers, L. H. (2020). The COVID-19 pandemic and the \$16 trillion virus. *JAMA*, 324(15), 1495–1496. <https://doi.org/10.1001/jama.2020.19759>
- Eaton, L. (2021). Covid-19: WHO warns against “vaccine nationalism” or face further virus mutations. *BMJ*, 372, n292. <https://doi.org/10.1136/bmj.n292>
- ESCAP. (2019). Asia-pacific disaster report 2019. Retrieved from <https://www.unescap.org/publications/asia-pacific-disaster-report-2019>
- Espitia, A., Rocha, N., & Ruta, M. (2020). *Covid-19 and food protectionism: The impact of the pandemic and export restrictions on world food markets*. The World Bank.
- Field, C. B., Barros, V., Stocker, T. F., & Dahe, Q. (2012). *Managing the risks of extreme events and disasters to advance climate change adaptation: Special report of the Intergovernmental Panel on Climate Change*. Cambridge University Press.
- Gohd, C. (2021). 2020 ties record for the hottest year ever, NASA analysis shows. Retrieved from <https://www.space.com/nasa-confirms-2020-hottest-year-on-record>
- Guan, D., Wang, D., Hallegatte, S., Davis, S. J., Huo, J., Li, S., Bai, Y., Lei, T., Xue, Q., Coffman, D., Cheng, D., Chen, P., Liang, X., Xu, B., Lu, X., Wang, S., Hubacek, K., & Gong, P. (2020). Global supply-chain effects of COVID-19 control measures. *Nature Human Behaviour*, 4(6), 577–587. <https://doi.org/10.1038/s41562-020-0896-8>
- Hallegatte, S. (2008). An adaptive regional input-output model and its application to the assessment of the economic cost of Katrina. *Risk Analysis*, 28(3), 779–799. <https://doi.org/10.1111/j.1539-6924.2008.01046.x>
- Hallegatte, S. (2014). Modeling the role of inventories and heterogeneity in the assessment of the economic costs of natural disasters. *Risk Analysis*, 34(1), 152–167. <https://doi.org/10.1111/risa.12090>
- Hao, Z., AghaKouchak, A., & Phillips, T. J. (2013). Changes in concurrent monthly precipitation and temperature extremes. *Environmental Research Letters*, 8(3), 034014. <https://doi.org/10.1088/1748-9326/8/3/034014>
- Hariri-Ardebili, M. A. (2020). Living in a multi-risk chaotic condition: Pandemic, natural hazards and complex emergencies. *International Journal of Environmental Research and Public Health*, 17(16), 5635. <https://doi.org/10.3390/ijerph17165635>
- Hsiang, S. M., & Jina, A. S. (2014). The causal effect of environmental catastrophe on long-run economic growth: Evidence from 6,700 cyclones (No. 20352). Retrieved from <https://www.nber.org/papers/w20352>
- Ishiwatari, M., Koike, T., Hiroki, K., Toda, T., & Katsube, T. (2020). Managing disasters amid COVID-19 pandemic: Approaches of response to flood disasters. *Progress in Disaster Science*, 6, 100096. <https://doi.org/10.1016/j.pdisas.2020.100096>
- Johnstone, W. M., & Lence, B. J. (2009). Assessing the value of mitigation strategies in reducing the impacts of rapid-onset, catastrophic floods.

- Journal of Flood Risk Management*, 2(3), 209–221. <https://doi.org/10.1111/j.1753-318X.2009.01035.x>
- Koks, E. E., Bočkarjova, M., de Moel, H., & Aerts, J. C. J. H. (2015). Integrated direct and indirect flood risk modeling: Development and sensitivity analysis. *Risk Analysis*, 35(5), 882–900. <https://doi.org/10.1111/risa.12300>
- Koks, E. E., & Thissen, M. (2016). A multiregional impact assessment model for disaster analysis. *Economic Systems Research*, 28(4), 429–449. <https://doi.org/10.1080/09535314.2016.1232701>
- Kuo, M. A. (2021). TSMC and Samsung: Semiconductor chip shortage. Retrieved from <https://thediplomat.com/2021/07/tsmc-and-samsung-semiconductor-chip-shortage/>
- Lackner, S. (2018). Earthquakes and economic growth (No. 190). Retrieved from <https://EconPapers.repec.org/RePEc:wsr:wpaper:y:2018:i:190>
- Laframboise, N., & Loko, B. (2012). Natural disasters: Mitigating impact, managing risks (No. 12/245). Retrieved from https://papers.ssrn.com/sol3/papers.cfm?abstract_id=2169784
- Lenzen, M., Malik, A., Kenway, S., Daniels, P., Lam, K. L., & Geschke, A. (2019). Economic damage and spillovers from a tropical cyclone. *Natural Hazards and Earth System Sciences*, 19(1), 137–151. <https://doi.org/10.5194/nhess-19-137-2019>
- Leonard, M., Westra, S., Phatak, A., Lambert, M., van den Hurk, B., McInnes, K., Risbey, J., Schuster, S., Jakob, D., & Stafford-Smith, M. (2014). A compound event framework for understanding extreme impacts. *Wiley Interdisciplinary Reviews: Climate Change*, 5(1), 113–128. <https://doi.org/10.1002/wcc.252>
- Li, J., Crawford-Brown, D., Syddall, M., & Guan, D. (2013). Modeling imbalanced economic recovery following a natural disaster using input-output analysis. *Risk Analysis*, 33(10), 1908–1923. <https://doi.org/10.1111/risa.12040>
- Mahul, O., & Signer, B. (2020). The perfect storm: How to prepare against climate risk and disaster shocks in the time of COVID-19. *One Earth*, 2(6), 500–502. <https://doi.org/10.1016/j.oneear.2020.05.023>
- McCarthy, N. (2021). The U.S. car models most impacted by the microchip shortage. Retrieved from <https://www.forbes.com/sites/niallmccarthy/2021/06/01/the-us-car-models-most-impacted-by-the-microchip-shortage-infographic/?sh=2cd3f50580d2>
- McKibbin, W. J., & Fernando, R. (2020). The global macroeconomic impacts of COVID-19: Seven scenarios (No. 19/2020). Retrieved from https://papers.ssrn.com/sol3/papers.cfm?abstract_id=3547729
- Mendoza-Tinoco, D., Hu, Y., Zeng, Z., Chalvatzis, K. J., Zhang, N., Steenge, A. E., & Guan, D. (2020). Flood footprint assessment: A multiregional case of 2009 Central European floods. *Risk Analysis*, 40(8), 1612–1631. <https://doi.org/10.1111/risa.13497>
- Miller, R. E., & Blair, P. D. (2009). *Input-output analysis: Foundations and extensions*. Cambridge University Press.
- Okuyama, Y., & Santos, J. R. (2014). Disaster impact and input-output analysis. *Economic Systems Research*, 26(1), 1–12. <https://doi.org/10.1080/09535314.2013.871505>
- Oosterhaven, J., & Többen, J. (2017). Wider economic impacts of heavy flooding in Germany: A non-linear programming approach. *Spatial Economic Analysis*, 12(4), 404–428. <https://doi.org/10.1080/17421772.2017.1300680>
- Oxford Analytica. (2020). Pandemic-induced trade protectionism will persist. *Expert Briefings*. <https://doi.org/10.1108/OXAN-ES257613>
- Pei, S., Dahl, K. A., Yamana, T. K., Licker, R., & Shaman, J. (2020). Compound risks of hurricane evacuation amid the COVID-19 pandemic in the United States. *GeoHealth*, 4(12), e2020GH000319. <https://doi.org/10.1029/2020GH000319>
- Phillips, C. A., Caldas, A., Cleetus, R., Dahl, K. A., Delet-Barreto, J., Licker, R., Merner, L. D., Ortiz-Partida, J. P., Phelan, A. L., Spanger-Siegfried, E., Talati, S., Trisos, C. H., & Carlson, C. J. (2020). Compound climate risks in the COVID-19 pandemic. *Nature Climate Change*, 10(7), 586–588. <https://doi.org/10.1038/s41558-020-0804-2>
- Reuters. (2020). Hyundai Motor suspends output as coronavirus disrupts supply chain. Retrieved from <https://www.reuters.com/article/hyundai-motor-virus-china-idUSS6N29P03H>
- Salas, R. N., Shultz, J. M., & Solomon, C. G. (2020). The climate crisis and Covid-19 – A major threat to the pandemic response. *New England Journal of Medicine*, 383(11), 70. <https://doi.org/10.1056/NEJMp2022011>
- Selby, D., & Kagawa, F. (2020). Climate change and coronavirus: A confluence of crises as learning moment. In P. Carmody, G. McCann, C. Colleran, & C. O'Halloran (Eds.), *COVID-19 in the global south: Impacts and responses*. Bristol University Press.
- Shahid, S. (2020). Deglobalization and its discontents: The pandemic effect. Retrieved from <https://economics.td.com/domains/economics.td.com/documents/reports/ss/deglobalization.pdf>
- Shen, X., Cai, C., Yang, Q., Anagnostou, E. N., & Li, H. (2021). The US COVID-19 pandemic in the flood season. *Science of the Total Environment*, 755, 142634. <https://doi.org/10.1016/j.scitotenv.2020.142634>
- Swaigood, M. (2020). When COVID-19 and natural hazards collide: Building resilient infrastructure in South Asia in the face of multiple crises. Retrieved from <https://www.orfonline.org/expert-speak/when-covid19-and-natural-hazards-collide/?MvBriefArticleId=18469>
- The Lancet Planetary Health. (2020). A tale of two emergencies. *The Lancet Planetary Health*, 4(3), e86. [https://doi.org/10.1016/S2542-5196\(20\)30062-0](https://doi.org/10.1016/S2542-5196(20)30062-0)
- Tripathy, S. S., Bhatia, U., Mohanty, M., Karmakar, S., & Ghosh, S. (2021). Flood evacuation during pandemic: A multi-objective framework to handle compound hazard. *Environmental Research Letters*, 16(3), 034034. <https://doi.org/10.1088/1748-9326/abda70>
- UNEP. (2020). Locust swarms and climate change. Retrieved from <https://www.unep.org/news-and-stories/story/locust-swarms-and-climate-change>
- UNFCCC. (2015). Adoption of the Paris Agreement (Report No. FCCC/CP/2015/L.9/Rev.1). Retrieved from United Nations Framework Convention on Climate Change, Paris, France: <http://unfccc.int/resource/docs/2015/cop21/eng/l09r01.pdf>
- UNISDR. (2015). Sendai framework for disaster risk reduction 2015–2030. Retrieved from United Nations International Strategy for Disaster Reduction, Sendai, Japan: http://www.wcdrr.org/uploads/Sendai_Framework_for_Disaster_Risk_Reduction_2015-2030.pdf
- White, D. A. L. (2020). 2020 Atlantic hurricane season most active on record. Retrieved from <https://www.msn.com/en-us/weather/topstories/2020-atlantic-hurricane-season-most-active-on-record-noaa/ar-BB1aStCW>
- WHO. (2015). Climate change and human health. Retrieved from <https://www.who.int/globalchange/global-campaign/cop21/en/>
- Willner, S. N., Otto, C., & Levermann, A. (2018). Global economic response to river floods. *Nature Climate Change*, 8(7), 594–598. <https://doi.org/10.1038/s41558-018-0173-2>
- World Bank. (2019). *World development report 2020: Trading for development in the age of global value chains*. The World Bank.
- World Trade Organization. (2020). Export prohibitions and restrictions. Retrieved from https://www.wto.org/english/tratop_e/covid19_e/export_prohibitions_report_e.pdf
- Xia, Y., Li, Y., Guan, D., Tinoco, D. M., Xia, J., Yan, Z., Yang, J., Liu, Q., & Huo, H. (2018). Assessment of the economic impacts of heat waves: A case study of Nanjing, China. *Journal of Cleaner Production*, 171, 811–819. <https://doi.org/10.1016/j.jclepro.2017.10.069>
- Yang, J., Xie, H., Yu, G., & Liu, M. (2021). Achieving a just-in-time supply chain: The role of supply chain intelligence. *International Journal of Production Economics*, 231, 107878. <https://doi.org/10.1016/j.ijpe.2020.107878>
- Zeng, Z., & Guan, D. (2020). Methodology and application of flood footprint accounting in a hypothetical multiple two-flood event. *Philosophical Transactions of the Royal Society A: Mathematical, Physical and Engineering Sciences*, 378(2168), 20190209. <https://doi.org/10.1098/rsta.2019.0209>
- Zeng, Z., Guan, D., Steenge, A. E., Xia, Y., & Mendoza-Tinoco, D. (2019). Flood footprint assessment: A new approach for flood-induced indirect economic impact measurement and post-flood recovery. *Journal of Hydrology*, 579, 124204. <https://doi.org/10.1016/j.jhydrol.2019.124204>

- Zhang, Z., Li, N., Cui, P., Xu, H., Liu, Y., Chen, X., & Feng, J. (2019). How to integrate labor disruption into an economic impact evaluation model for postdisaster recovery periods. *Risk Analysis*, 39(11), 2443–2456. <https://doi.org/10.1111/risa.13365>
- Zheng, H., Zhang, Z., Wei, W., Song, M., Dietzenbacher, E., Wang, X., Meng, J., Shan, Y., Ou, J., & Guan, D. (2020). Regional determinants of China's consumption-based emissions in the economic transition. *Environmental Research Letters*, 15(7), 074001. <https://doi.org/10.1088/1748-9326/ab794f>
- Zscheischler, J., Westra, S., van den Hurk, B. J. J. M., Seneviratne, S. I., Ward, P. J., Pitman, A., AghaKouchak, A., Bresch, D. N., Leonard, M., Wahl, T., & Zhang, X. (2018). Future climate risk from compound events. *Nature Climate Change*, 8(6), 469–477. <https://doi.org/10.1038/s41558-018-0156-3>

How to cite this article: Hu, Y., Wang, D., Huo, J., Chemutai, V., Brenton, P., Yang, L., & Guan, D. (2023). Assessing the economic impacts of a perfect storm of extreme weather, pandemic control, and export restrictions: A methodological construct. *Risk Analysis*, 1–35. <https://doi.org/10.1111/risa.14146>

APPENDIX A: SUPPLEMENTARY METHODS

This section provides supplementary information about the pre-disaster economic equilibrium, perfect storm-induced external shocks to the economy, and prioritized-proportional rationing scheme under export restrictions in our compound-hazard impact model.

A.1 | Pre-disaster economic equilibrium

Initially, under the equilibrium conditions, the output of sector i in region r is equal to the aggregate demand for its products from both downstream sectors and households over all regions, as follows:

$$\bar{x}_{ir} = \sum_{s=1}^R \sum_{j=1}^P a_{ir-js} \times \bar{x}_{js} + \sum_{h=1}^R \bar{hd}_{ir,h}, \quad (\text{A.1})$$

where \bar{x}_{ir} denotes the output of product i in region r in the equilibrium state. We use overbars to indicate values at the pre-disaster equilibrium levels. The first summation on the right-hand side represents the intermediate demand for product i in region r from downstream sectors. a_{ir-js} refers to the amount of product i in region r required to produce one unit of product j in region s , which can be derived from the input–output matrix. The second summation calculates the final demand from households. $\bar{hd}_{ir,h}$ is the equilibrium quantity of product i produced in region r and consumed by the household in region h .

The above equilibrium breaks up following a pandemic-induced perfect storm, which triggers direct and knock-on effects on the whole economic system.

A.2 | External shocks introduced by a perfect storm to labor, transport, export, and final demand

Labor damage

Labor damage induced by the perfect storm is twofold. First, it increases the number of employees unable to work because of injury, illness, or death from flooding or virus infection. Second, employees also spend less time working due to the damage to transport infrastructure and services during the event. Therefore, labor damage, $\gamma_{ir}^L(t)$, is expressed as the fraction of working hour loss in each sector and region during each time step:

$$\gamma_{ir}^L(t) = \frac{(L_{ir}^C(t) + L_{ir}^F(t)) \times \bar{wh}_{ir} + [\bar{L}_{ir} - L_{ir}^C(t) - L_{ir}^F(t)] \times \Delta wh_{ir}(t)}{\bar{L}_{ir} \times \bar{wh}_{ir}}, \quad (\text{A.2})$$

where \bar{L}_{ir} and \bar{wh}_{ir} represent the number of employees and working hours per capita of sector i in region r at the pre-disaster levels. $L_{ir}^C(t)$ and $L_{ir}^F(t)$ are the numbers of workers unable to work due to virus infection and flooding at time t , respectively. $\Delta wh_{ir}(t)$ is the loss of working hours per capita in sector i in region r at time t . It is determined by the degree of transport disruption in region r , $\gamma_r^Z(t)$, as defined in Section A.2.2, and a sector-specific impact multiplier, η_i :

$$\Delta wh_{ir}(t) = \eta_i \times \gamma_r^Z(t) \times \bar{wh}_{ir}, \quad (\text{A.3})$$

where η_i captures the impact of transport disruption on the operation of sector i . It is based on three factors: the degree of exposure of the sector (e.g., the extent of in-person interactions), whether it is the lifeline sector (e.g., electricity) and the possibility for work at home (Guan et al., 2020). For example, the multiplier for the education sector could be low (e.g., 0.1) because of the development of online learning.

Transport disruption

The pandemic control and flooding have different but parallel impacts on the transportation system. For one thing, restrictions on public transport are placed in the epidemic regions to contain virus transmission. Those restrictions may include reducing the number of passengers to keep social distance and suspending international flights from epidemic areas. We use $\gamma_r^{Z,C}(t)$ to denote the percentage by which transportation capacity is reduced by lockdown measures relative to the equilibrium levels in region r at time t , a metric for the strictness of pandemic control. Second, the transport infrastructure (e.g., roads, railways, and airports) may be inundated and out of operation in flooded regions. We use $\gamma_r^{Z,F}(t)$ to represent the percentage of submerged transport infrastructure during flooding. We assume that the transport capacity from region r to region s is simply constrained by the transport conditions in region r , which is further determined by the severer one between epidemic and flooding constraints in that region. Therefore, the relative reduction of transport capacity from

region r to region s at time t , $\gamma_{r,s}^Z(t)$, is calculated as

$$\gamma_{r,s}^Z(t) = \gamma_r^Z(t) = \max \left\{ \gamma_{r,s}^{Z,C}(t), \gamma_{r,s}^{Z,F}(t) \right\}. \quad (\text{A.4})$$

The impacts of transport disruption are twofold. First, it affects labor supply as mentioned above. Second, it increases the difficulty in delivering the intermediate and final products to downstream sectors and households. Similar to the labor constraint, we define the connectivity losses between supply and demand in different regions as follows:

$$\gamma_{ir,js}^Z(t) = \eta_i \times \gamma_{r,s}^Z(t) \quad (\text{A.5})$$

and

$$\gamma_{ir,h}^Z(t) = \eta_i \times \gamma_{r,h}^Z(t), \quad (\text{A.6})$$

where the connectivity losses, $\gamma_{ir,js}^Z(t)$ and $\gamma_{ir,h}^Z(t)$, are expressed by the relative reductions in the capacity to transport the product of sector i in region r to sector j in region s and to the household in region h , respectively, at time t .

Export restrictions

With the ongoing process of deglobalization, particularly in the complex pandemic and natural crises, export restrictions may be imposed by countries/regions on critical products (e.g., food and medical gear). Although the export restrictions applied by large exporters may in the short run increase domestic availability, the measures reduce the world's supply of the products concerned, and the importing countries incapable of self-sufficiency will suffer (World Trade Organization, 2020). We use $\gamma_{ir}^E(t)$ to denote the degree of export restrictions introduced by region r on product i at time t . It is measured by the percentage reduction of the maximum export volume of that product in region r relative to the pre-disaster level.

Final demand shock

Finally, households adjust their consumption in response to the perfect storm. For example, they spend more time in staying at home and less money on eating out, hotels, and other outdoor entertainment. Households in disasters also show a propensity for stocking medical and emergency products, such as medicine, masks, and life jackets. We assume that the local consumption, import and export of the accommodation, and food and recreation services decline by $\alpha\%$ in the epidemic and flooded regions, whereas the local consumption and import of medical services and emergency products increase by $\beta\%$ in these regions. This adaptive behavior of households is expressed as

$$hd_{ir,h}(t) = (1 - \alpha\%)^{I(i \in \Omega_\alpha) \times I(r, h \in R_C \cup R_F)} \times (1 + \beta\%)^{I(i \in \Omega_\beta) \times I(h \in R_C \cup R_F)} \times \overline{hd}_{ir,h}, \quad (\text{A.7})$$

where $hd_{ir,h}(t)$ refers to the consumption of the household in region h for product i in region r at time t . $I(i \in \Omega_\alpha)$ is the indicator function that takes value 1 when product i belongs to the sector set of accommodation, food, and recreation services (Ω_α), otherwise it takes value 0. $I(r, h \in R_C \cup R_F)$ is the indicator function that takes value 1 when region r or h is one of the epidemic regions (R_C) or flooded regions (R_F), otherwise it takes value 0. Similarly, $I(i \in \Omega_\beta)$ is the indicator function that takes value 1 when product i belongs to the sector set of medical services and emergency products (Ω_β), otherwise it takes value 0. $I(h \in R_C \cup R_F)$ is the indicator function which takes value 1 when region h is one of the epidemic or flooded regions, otherwise it takes value 0.

A.3 | Prioritized-proportional rationing scheme under export restrictions

First, products made by sector i in region r are allocated to sector j in region s in quantities, $FRC_{js}^{ir}(t)$, as follows:

$$FRC_{js}^{ir}(t) = \begin{cases} \frac{FOD_{js}^{ir}(t-1)}{\sum_{s=1}^R \sum_{j=1}^P FOD_{js}^{ir}(t-1)} \times x_{ir}^d(t), & \text{if } x_{ir}^d(t) < \sum_{s=1}^R \sum_{j=1}^P FOD_{js}^{ir}(t-1) \\ FOD_{js}^{ir}(t-1), & \text{if } x_{ir}^d(t) \geq \sum_{s=1}^R \sum_{j=1}^P FOD_{js}^{ir}(t-1) \end{cases}, \quad (\text{A.8})$$

where $FOD_{js}^{ir}(t-1)$ refers to the order issued by sector j in region s to its supplier of sector i in region r at time $t-1$. If the actual output of sector i in region r is smaller than its expected total orders from downstream sectors, that is, $\sum_{s=1}^R \sum_{j=1}^P FOD_{js}^{ir}(t-1)$, it will allocate all its output to the business clients in proportion to the orders. Otherwise, it will allocate just enough products to satisfy the expected intermediate demand.

The remaining products of sector i in region r , after satisfying the intermediate demand, at time step t , is equal to

$$x_{ir}^{rem}(t) = x_{ir}^d(t) - \sum_{s=1}^R \sum_{j=1}^P FRC_{js}^{ir}(t). \quad (\text{A.9})$$

Then, the remaining products will be proportionally allocated to the final demand and reconstruction demand, respectively. The quantities allocated to the household in region h , $HRC_h^{ir}(t)$, and the reconstruction agent of sector j in region s , $RRC_{js}^{ir}(t)$, are

$$HRC_h^{ir}(t) = \frac{HOD_h^{ir}(t-1)}{\sum_{h=1}^R HOD_h^{ir}(t-1) + \sum_{s=1}^R \sum_{j=1}^P ROD_{js}^{ir}(t-1)} \times x_{ir}^{rem}(t) \quad (\text{A.10})$$

and

$$RRC_{js}^{ir}(t) = \frac{ROD_{js}^{ir}(t-1)}{\sum_{h=1}^R HOD_h^{ir}(t-1) + \sum_{s=1}^R \sum_{j=1}^P ROD_{js}^{ir}(t-1)} \times x_{ir}^{rem}(t), \quad (\text{A.11})$$

where $HOD_h^{ir}(t-1)$ refers to the order issued by the household h , and $ROD_{js}^{ir}(t-1)$ refers to the order issued to rebuild damaged capital of sector j in region s , to the supplier of sector i in region r at time $t-1$.

The allocation of outputs should also be subject to the export restrictions, which means that the total export of a sector at each time step should be no more than its maximum quota restricted by the trade policy:

$$\sum_{s \neq r} \sum_{j=1}^P FRC_{js}^{ir}(t) + \sum_{h \neq r} HRC_h^{ir}(t) + \sum_{s \neq r} \sum_{j=1}^P RRC_{js}^{ir}(t) \leq (1 - \gamma_{ir}^E(t)) \times \bar{e}x_{ir}, \quad (\text{A.12})$$

where $\gamma_{ir}^E(t)$ is the degree of export restriction imposed on product i by region r at time t . It is measured by the percentage reduction of the maximum export volume of that product in region r relative to the pre-disaster level (see Section A.2.3). $\bar{e}x_{ir}$ represents the export volume of this product at the pre-disaster equilibrium level.

We adjust the export of sector i in region r to downstream sectors, $FRC_{js}^{ir}(t)$, to households, $HRC_h^{ir}(t)$, and to reconstruction activities, $RRC_{js}^{ir}(t)$, where $s, h \neq r$, to satisfy the constraint (Equation A.12) according to a similar prioritized-proportional rationing scheme. Specifically, the output allocated to the downstream sector j in region s ($s \neq r$) after adjustment to the export restriction, $FRC_{js}^{ir,*}(t)$, is equal to

$$FRC_{js}^{ir,*}(t) = \begin{cases} \frac{FRC_{js}^{ir}(t)}{\sum_{s \neq r} \sum_{j=1}^P FRC_{js}^{ir}(t)} \times (1 - \gamma_{ir}^E(t)) \times \bar{e}x_{ir}, & \text{if } \sum_{s \neq r} \sum_{j=1}^P FRC_{js}^{ir}(t) > (1 - \gamma_{ir}^E(t)) \times \bar{e}x_{ir}, \\ FRC_{js}^{ir}(t), & \text{if } \sum_{s \neq r} \sum_{j=1}^P FRC_{js}^{ir}(t) \leq (1 - \gamma_{ir}^E(t)) \times \bar{e}x_{ir} \end{cases}, \quad (\text{A.13})$$

Here we still assume that the intermediate demands of downstream sectors are given the priority to be satisfied under export restriction. The asterisk stands for the adjusted value according to export restrictions.

Afterward, the remaining export quota, $exq_{ir}^{rem}(t)$, is

$$exq_{ir}^{rem}(t) = (1 - \gamma_{ir}^E(t)) \times \bar{e}x_{ir} - \sum_{s \neq r} \sum_{j=1}^P FRC_{js}^{ir,*}(t). \quad (\text{A.14})$$

Then the remaining export quota is allocated to the final and reconstruction demands, as follows:

$$HRC_h^{ir,*}(t) = \begin{cases} \frac{HRC_h^{ir}(t)}{\sum_{h \neq r} HRC_h^{ir}(t) + \sum_{s \neq r} \sum_{j=1}^P RRC_{js}^{ir}(t)} \times exq_{ir}^{rem}(t), & \text{if } \sum_{h \neq r} HRC_h^{ir}(t) + \sum_{s \neq r} \sum_{j=1}^P RRC_{js}^{ir}(t) > exq_{ir}^{rem}(t), \\ HRC_h^{ir}(t), & \text{if } \sum_{h \neq r} HRC_h^{ir}(t) + \sum_{s \neq r} \sum_{j=1}^P RRC_{js}^{ir}(t) \leq exq_{ir}^{rem}(t) \end{cases}, \quad \text{for } h \neq r \quad (\text{A.15})$$

and

$$RRC_{js}^{ir,*}(t) = \begin{cases} \frac{RRC_{js}^{ir}(t)}{\sum_{h \neq r} HRC_h^{ir}(t) + \sum_{s \neq r} \sum_{j=1}^P RRC_{js}^{ir}(t)} \times exq_{ir}^{rem}(t), & \text{if } \sum_{h \neq r} HRC_h^{ir}(t) + \sum_{s \neq r} \sum_{j=1}^P RRC_{js}^{ir}(t) > exq_{ir}^{rem}(t), \\ RRC_{js}^{ir}(t), & \text{if } \sum_{h \neq r} HRC_h^{ir}(t) + \sum_{s \neq r} \sum_{j=1}^P RRC_{js}^{ir}(t) \leq exq_{ir}^{rem}(t) \end{cases}, \quad \text{for } s \neq r. \quad (\text{A.16})$$

After export adjustment, the remaining output of sector i in region r available for local clients, $x_{ir}^{loc}(t)$, is calculated as

$$x_{ir}^{loc}(t) = x_{ir}^a(t) - \sum_{s \neq r} \sum_{j=1}^P FRC_{js}^{ir,*}(t) - \sum_{h \neq r} HRC_h^{ir,*}(t) - \sum_{s \neq r} \sum_{j=1}^P RRC_{js}^{ir,*}(t). \quad (\text{A.17})$$

Finally, the products of sector i in region r allocated to the local sectors, household, and reconstruction agents are adjusted proportionally as follows:

$$FRC_{jr}^{ir,*}(t) = \frac{FRC_{jr}^{ir}(t)}{FRC_{jr}^{ir}(t) + HRC_r^{ir}(t) + RRC_{jr}^{ir}(t)} \times x_{ir}^{loc}(t), \quad (\text{A.18})$$

$$HRC_r^{ir,*}(t) = \frac{HRC_r^{ir}(t)}{FRC_{jr}^{ir}(t) + HRC_r^{ir}(t) + RRC_{jr}^{ir}(t)} \times x_{ir}^{loc}(t), \quad (\text{A.19})$$

and

$$RRC_{jr}^{ir,*}(t) = \frac{RRC_{jr}^{ir}(t)}{FRC_{jr}^{ir}(t) + HRC_r^{ir}(t) + RRC_{jr}^{ir}(t)} \times x_{ir}^{loc}(t). \quad (\text{A.20})$$

A.4 | List of key variables

TABLE A.1 List of key variables

Variables	Definitions
R	Number of regions in the world economy
R^i	Set of regions supplying product i
P	Number of production sectors making unique products
Q	Number of specialized products
$a_{j,ir}$	Intermediate input j required to produce one unit of product i in region r
$b_{k,ir}$	Primary input k required to produce one unit of product i in region r
d_{js}^{ir}	Product i in region r invested in one unit of capital formation of sector j in region r
n_{ir}^j	Weeks of intermediate use of inventory product j that sector i in region r wants to hold
α_{ir}^{\max}	Maximum overproduction capacity of sector i in region r relative to the pre-disaster level
τ_α	Weeks needed by a sector to achieve its maximum overproduction capacity
\bar{ex}_{ir}	Export of product i from region r to other regions under the pre-disaster equilibrium state
$x_{ir}^a(t)$	Actual output of sector i in region r at time t
$x_{ir}^{\max}(t)$	Maximum production capacity of sector i in region r at time t
$va_{ir}(t)$	Value added of sector i in region r at time t
$K_{ir}(t)$	Capital stock of sector i in region r at time t
$K_{ir}^F(t)$	Capital damaged by flooding of sector i in region r at time t
$K_{ir}^{REC}(t)$	Capital recovered of sector i in region r from reconstruction at the end of time t
$\gamma_{ir}^K(t)$	Percentage reduction in capital stock of sector i in region r at time t relative to the pre-disaster level
$\gamma_{ir}^L(t)$	Fraction of working hour loss in sector i in region r at time t
$\gamma_{ir,js}^Z(t)$	Relative reduction in the capacity to transport the product of sector i in region r to sector j in region s at time t
$\gamma_{ir,h}^Z(t)$	Relative reduction in the capacity to transport the product of sector i in region r to the household in region h at time t
$\gamma_{ir}^E(t)$	Degree of export restriction imposed on product i by region r at time t
$S_{ir}^j(t)$	Inventory of intermediate input j held by sector i in region r at the end of time t
$S_{ir}^{j,used}(t)$	Intermediate input j used in the production of sector i in region r at time t
$S_{ir}^{j,restored}(t)$	Inventory of intermediate input j restored by sector i in region r at time t
$S_{ir}^{j,G}(t)$	Targeted inventory level of intermediate input j held by sector i in region r at time t
$FRC_{js}^{ir,*}(t)$	Output of sector i in region r allocated to sector j in region s as intermediate use at time t under export restrictions
$HRC_h^{ir,*}(t)$	Output of sector i in region r allocated to household in region h as consumption use at time t under export restrictions
$RRC_{js}^{ir,*}(t)$	Output of sector i in region r allocated to sector j in region s as reconstruction use at time t under export restrictions
$FOD_{js}^{ir}(t)$	Orders issued by sector j in region s to the supplier of sector i in region r at time t
$HOD_h^{ir}(t)$	Orders issued by the household in region h to the supplier of sector i in region r at time t
$ROD_{js}^{ir}(t)$	Orders issued to rebuild damaged capital of sector j in region s to the supplier of sector i in region r at time t
$TD_{ir}(t)$	Total demand of product i in region r at time t

TABLE B.3 Capital matrix^a

Region-Sector	A	B	C	D	
A	AGR	0	0	0	0
	MANG	0	0	0	0
	MANR	0.15	0	0.02	0
	CON	0.61	0	0	0
	OTH	0	0	0	0
B	AGR	0	0	0	0
	MANG	0	0	0	0
	MANR	0.06	0.25	0.06	0
	CON	0.12	0.7	0.04	0
	OTH	0	0	0	0
C	AGR	0	0	0	0
	MANG	0	0	0	0
	MANR	0.02	0.05	0.2	0
	CON	0.04	0	0.68	0
	OTH	0	0	0	0
D	AGR	0	0	0	0
	MANG	0	0	0	0
	MANR	0	0	0	0.3
	CON	0	0	0	0.7
	OTH	0	0	0	0

^aThe matrix presents the quantities of products required to rebuild one unit of capital in each region. We assume that different sectors in the same region have the same capital matrix coefficients.

APPENDIX C: SUPPLEMENTARY RESULTS

C.1 | Direct and indirect impacts under free trade scenarios

This section discusses the direct and indirect economic impacts of flooding, pandemic control, and their collision under the free trade scenarios. The direct damage refers to the monetary value of damage due to inundation of physical assets and occurs only in the flooded region C. The indirect losses are the GDP losses along the global supply chain caused by the compound event. They start from the directly affected regions and spill over to other regions through inter-sectoral and inter-regional dependencies.

On the global scale

As shown in Table 3, when there is only flooding in region C, the direct damage increases from 317.2 to 951.5 units as the flood scale grows from small to large. Apart from direct damage, the flood disaster brings about additional supply chain losses of 50.0–288.9 units according to flood scales. The ratios between indirect and direct losses range from 0.16 to 0.30 as flood scale increases and are lower than the ratio of 0.39 estimated by Hallegatte (2008). This is because the incorporation of cross-regional substitutability increases the resilience of the economy against disastrous events and reduces estimates of indirect losses.

In the scenario where there is only pandemic control, there is no direct damage as the pandemic has no impact on physical assets. The indirect losses due to a 30%–24 global pandemic control are assessed at 1242.6 units, equivalent to 12.9% of the annual global GDP.

Then we examine the economic footprint of the compound event of flooding and pandemic control. The direct damage under such circumstances is always equal to that caused by flooding alone, as the pandemic does not create any direct damage. The indirect losses resulting from the compound events show diverging patterns according to flood scales. First, when the flood in region C is on the small or medium scale, the indirect losses of the compound event are between the separate losses brought by flooding and pandemic control. For example, the concurrence of a small flood in region C and a 30%–24 global pandemic control incurs 1194.1 units of indirect losses to the global economy, which is larger than the indirect losses caused by the flood (50.0 units) and slightly smaller than the indirect losses of the pandemic control (1242.6 units). Second, when the flood in region C is on the large scale, the indirect losses of the compound event, which is measured at 1329.5 units, exceed the separate losses of both flooding and pandemic control.

On the regional scale

As shown in Figure 2, under the flood-only scenario (Figure 2a–c), the cumulative indirect or GDP losses in region C (yellow lines), relative to its pre-disaster level of its annual GDP, increase from 2.18% (small flood), to 6.41% (medium flood), and finally to 12.25% (large flood). Region D also experiences increasing losses in its GDP, although very tiny (0.01%–0.05%), attributable to the spill-over effects along the supply chain. By contrast, the other two non-flooded regions A and B witness slight growth in their GDPs (0.07%–0.34% for A and 0.21%–0.98% for B). This comes from the stimulus effect of reconstruction activities to recover capital damaged by flooding, which has been discussed in the main text.

Figure 2d–f shows the regional economic footprint of the pandemic control, which is irrelevant to the flood scales. The four regions experience similar weekly relative changes in their GDPs during a 30%–24 global pandemic control. Their GDPs drop gradually by around 22% during the first 3 weeks (weeks 5–8) of the pandemic control, then remain almost constant for the remaining weeks of the pandemic control, and finally recover back to the pre-disaster levels when the control measures are lifted. The recovery takes another around 10 weeks in all regions. Before that, there are sudden slumps of regional GDPs around week 30, due to the shortage of intermediate inputs arising from delivery failures under persistent transport constraints during the pandemic control. The cumulative GDP losses in regions A–D caused by a 30%–24 pandemic control account for 12.61%, 12.87%, 13.20%, and 13.04% of their annual GDP at the pre-pandemic levels.

Figure 2g–i illustrates the regional losses resulting from the perfect storm of flooding and pandemic control. It takes longer weeks in region C to recover its economy compared to the above two groups of scenarios, particularly with the large

TABLE C.1 Changes in cumulative GDP losses on regional and global scales by each 25% increase in the degree of the export restriction on “MANR-C” without production specialization^a

Export restriction (%)	Region A (%)	Region B (%)	Region C (%)	Region D (%)	Global change (%)
0–25	0.08	0.00	−0.03	0.06	0.02
25–50	0.35	0.17	−0.03	0.39	0.18
50–75	0.38	0.21	−0.03	0.52	0.22

^aThe cumulative GDP losses are in relative terms of the annual GDPs at the pre-disaster levels. The results are given as the ensemble mean of scenarios where different scales of floods collide with a 30%–24 pandemic control.

flood scale. The cumulative GDP losses in region C increase significantly with the flood scale from 12.11% to 18.75%. By comparison, other regions experience different levels of declines in their GDP losses as the flood scale increases (12.41%–12.00% for A, 12.49%–11.56% for B, and 12.96%–12.86% for D), owing to an expanding stimulus effect of post-flood reconstruction.

C.2 | Economic impacts of different degrees of export restrictions

In this section, we investigate how the economic impacts of the perfect storm change with the degree of the trade restriction limiting the export of sector “MANR” in region C. We assume that the degree of the export restriction increases from 0% to 75% with an interval of 25%.

First, Table C.1 illustrates the changes in cumulative GDP losses, both on the regional and global scales, by the export restriction without production specialization, that is, products in one region can be freely replaced by products of the same sector from other regions. We find that not only the global loss but also its increment expands with the degree of the export restriction. In other words, a stronger export restriction results in a larger increase in the GDP loss than a weaker one. For every 25% increase in the degree of the export restriction, the global loss rises by an average of 0.02%, 0.18%, and 0.22%, respectively, during different flood and pandemic intersections. The GDP loss in each region, except region C, follows the same pattern as the global one with increases in the degree of the export restriction. In comparison, regions A and D appear to be more vulnerable to the escalating trade restriction than other regions. In region C, its loss increases by 0.01% with each 25% increase in the degree of the export restriction under the small flood colliding with pandemic control but decreases by 0.03% and 0.07%, respectively, under the medium and large floods (Figure C.1).

Second, we examine the role of production specialization in compound scenarios with varying degrees of the export restriction on “MANR-C.” As shown in Table C.2 and Figure C.2, the regional and global GDP losses both grow rapidly with the degree of the export restriction when the restricted sector “MANR-C” happens to make specialized products that cannot be substituted elsewhere. Such restrictive policy of region C puts other regional economies, as well as the global economy, at considerably higher risks than the former one, which in turn damages its own recovery through the propagation effect of the global supply chain.

These results are consistent with those of Section 3.2 in the main text.

C.3 | Sensitivity analysis

We perform a sensitivity analysis on key parameters, mainly about the inventory and overproduction adjustment, to check the robustness of modeling results. We examine how the regional and global indirect impacts (i.e., losses of GDP relative to the pre-disaster levels), which are caused by a perfect storm, change with these parameters. For simplicity, we only demonstrate a typical compound scenario covering triple shocks, that is, region C, which is hit by a large flood, restricts the export of its “MANR” sector by 50%, and region B imposes retaliatory restriction on the same sector by the same degree during a 30%–24 pandemic control. The reference results are illustrated in Table 6 and Figure 4i in the main text. Here we do not consider the possibility of production specialization to avoid extreme simulations that may obscure the variability of results.

Finally, we examine how economic losses, as well as our main findings, change if we use a different multiregional Input–Output (MRIO) table to construct the hypothetical global economy. The new MRIO table is obtained from an aggregated 2014 version of GTAP 10 Data Base (Aguilar et al., 2019), still consisting of four regions and the same five sectors. We scale the new table to keep the global annual GDP the same as in the main text (9613 units), but the proportion that each region accounts for is changed, that is, 24% for region A, 29% for region B, 25% for region C, and 22% for region D (Table B.2).

Inventory size

As explained in Section 2.4.1, the targeted inventory size of each sector before and after the compound shock is defined by the parameter n_{js}^i . Figure C.3 shows that model results are quite sensitive to this parameter, notably with regions A and D. Increasing inventory size can help improve economic resilience by lowering the risk of inventory shortage amid negative shocks. For instance, the production constraint resulting from an inventory shortage in region A is delayed from weeks 10 to 31 as the inventory size increases from 2 to 8 weeks, and there is no more such reduction in production when the inventory size is larger than or equal to 10 weeks. Globally, the cumulative GDP losses resulting from the perfect storm decrease from 18.1% to 12.5% as the inventory size increases from 2 to 12 weeks.

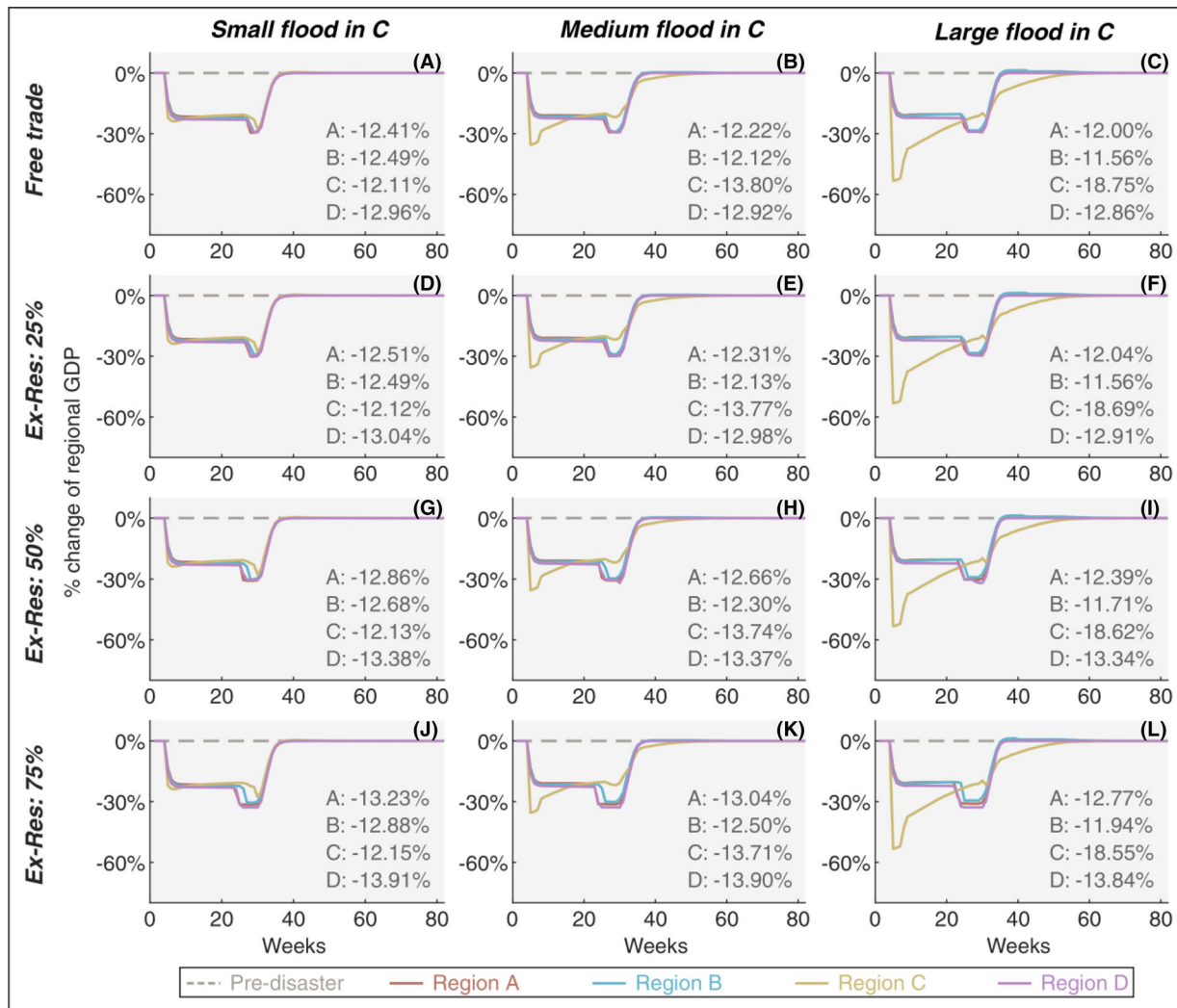


FIGURE C.1 Weekly changes of regional GDPs, relative to the pre-disaster level, in the four regions, when the export restriction is imposed on “MANR-C” at different degrees without production specialization during the compound flood and pandemic crises. The numbers in each plot indicate the cumulative losses or gains of regional GDPs over time, relative to the pre-disaster levels of the annual regional GDPs. From left to right, each column represents the small-, medium-, and large-scale flooding in region C. From top to bottom, each row stands for the 0%, 25%, 50%, or 75% export restriction on the “MANR” sector in region C.

TABLE C.2 Changes in cumulative GDP losses on regional and global scales by each 25% increase in the degree of the export restriction on “MANR-C” with production specialization^a

Export restriction (%)	Region A (%)	Region B (%)	Region C (%)	Region D (%)	Global change (%)
0–25	7.26	7.27	0.56	6.56	5.30
25–50	9.46	9.38	1.17	9.41	7.09
50–75	9.87	9.85	1.05	9.86	7.38

^aThe cumulative GDP losses are in relative terms of the annual GDPs at the pre-disaster levels. The results are given as the ensemble mean of scenarios where different scales of floods collide with a 30%–24 pandemic control.

Inventory restoration rate

Dynamic instabilities, or the so-called bullwhip effect, may sometimes set in when sectors try to restore their inventories too quickly. To address these instabilities, although not encountered in the main text, we could introduce a new

parameter τ_s to control the speed of inventory restoration. It describes the proportion of inventory losses that economic sectors try to restore in the next time step. For instance, if they lose x unit of their inventory, compared to the pre-disaster level, then they will increase their intermediate order

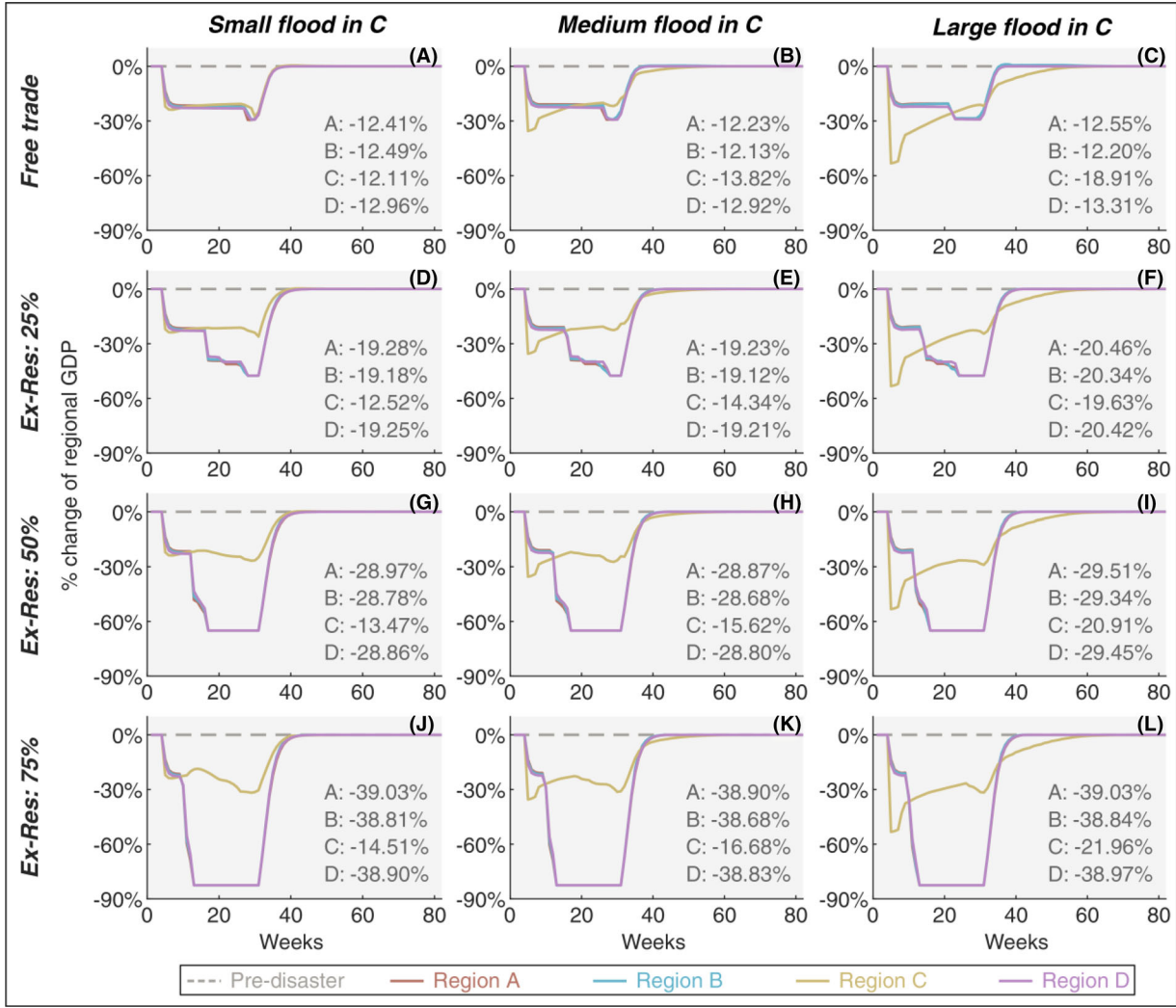


FIGURE C.2 Weekly changes of regional GDPs, relative to the pre-disaster level, in the four regions, when the export restriction is imposed on “MANR-C” at different degrees with production specialization during the compound flood and pandemic crises. The numbers in each plot indicate the cumulative losses or gains of regional GDPs over time, relative to the pre-disaster levels of the annual regional GDPs. From left to right, each column represents the small-, medium-, and large-scale flooding in region C. From top to bottom, each row stands for the 0%, 25%, 50%, or 75% export restriction on the “MANR” sector in region C.

by $\tau_s \times x$ unit right in the next time step, and $0 \leq \tau_s \leq 1$. Therefore, the order made by sector j in region s for intermediate input of product i at time t is calculated as follows:

$$FOD_{js}^i(t) = \tau_s \times \left(S_{js}^{i,G}(t) - S_{js}^i(t) - a_{ijs} \times \bar{x}_{js} \right) + a_{ijs} \times \bar{x}_{js}, \tag{C.1}$$

where $S_{js}^{i,G}(t) - S_{js}^i(t)$ is the gap between targeted and actual inventory levels at time t , and $a_{ijs} \times \bar{x}_{js}$ is that gap at the pre-disaster level. The latter is also the intermediate orders made each time before the disaster.

In the main text, τ_s is equal to 1, and $FOD_{js}^i(t) = S_{js}^{i,G}(t) - S_{js}^i(t)$.

Then the order issued by sector j in region s to its supplier of sector i in region r is

$$FOD_{js}^{ir}(t) = \begin{cases} FOD_{js}^i(t) \times \frac{\overline{FOD}_{js}^{ir} \times (1 - \gamma_{ir,js}^Z(t)) \times (1 - \gamma_{ir}^E(t)) \times x_{ir}^a(t)}{\sum_{r \in R^i} \overline{FOD}_{js}^{ir} \times (1 - \gamma_{ir,js}^Z(t)) \times (1 - \gamma_{ir}^E(t)) \times x_{ir}^a(t)}, & \text{if } FOD_{js}^i(t) > 0 \\ 0 & \text{if } FOD_{js}^i(t) \leq 0, \end{cases} \tag{C.2}$$

which corresponds to Equation (17) in the main text.

Figure C.4 illustrates how the regional and global economic losses change with five different values of inventory

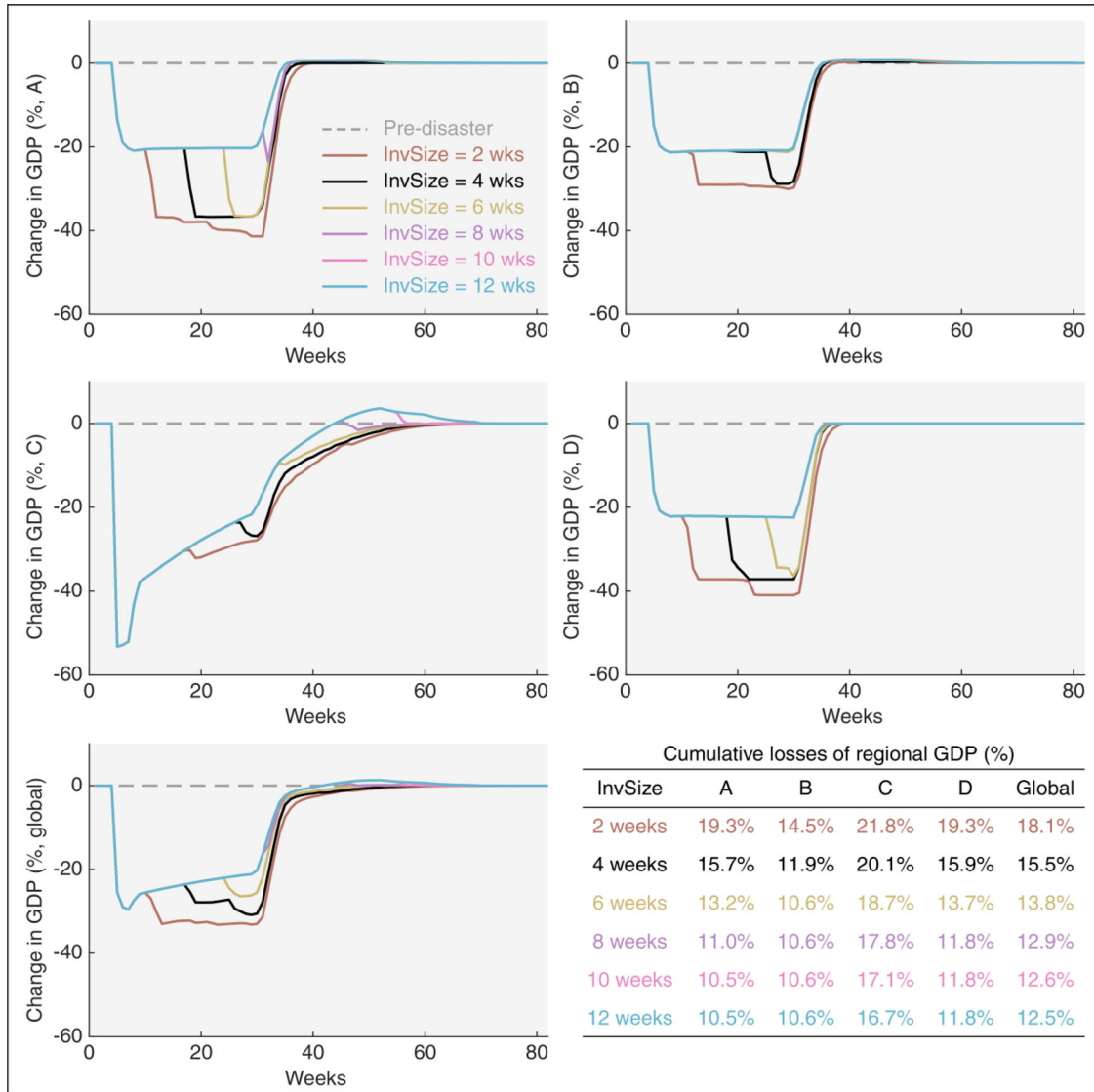


FIGURE C.3 Weekly changes in regional and global GDPs, relative to their pre-disaster levels, for the six values of inventory size, during the perfect storm of flooding, pandemic control, and export restrictions. The first four plots illustrate the robustness of results in regions A–D, respectively, and the last plot stands for the global economy. The table at the bottom right presents the cumulative losses of regional and global GDPs, relative to the pre-disaster annual levels, for the six values of inventory size.

restoration rate. In general, these losses are less sensitive to the inventory restoration rate than the inventory size. Although lowering the inventory restoration rate may spare more goods for reconstruction and other final demands, it accelerates the occurrence of inventory shortages and finally slows down the whole recovery process. The economic losses in regions A, B, and D grow by roughly 1% when the inventory restoration rate is cut from 1 to 0.2. By contrast, the loss in region C, which is hit by the flood, is the least sensitive to this parameter, reaching its lowest when the inventory restoration rate is between 0.4 and 0.6.

Maximum overproduction capacity

As explained in Section 2.4.4, the overproduction module describes how economic sectors, particularly those involved in reconstruction, adapt their production capacity to an

increasing demand for post-disaster recovery. It introduces two important parameters: the maximum overproduction capacity α_{ir}^{\max} and the overproduction adjustment time τ_{α} .

We first examine the result robustness to the first parameter α_{ir}^{\max} , which defines the upper limit of overproduction capacity. As shown in Figure C.5, the economic recovery of region C is much more sensitive to this parameter than that of other regions. This is not surprising as region C is the only region hit by the flood. When the maximum overproduction capacity is large, the production in sectors involved in reconstruction (i.e., the “MANR” and “CON” sectors) soars to address the increasing need for reconstruction, which offsets some of the output loss in other sectors. The economic losses in regions A and B also decrease slightly with the increase in maximum overproduction capacity, as some of their products are needed by region C for reconstruction. Globally, the

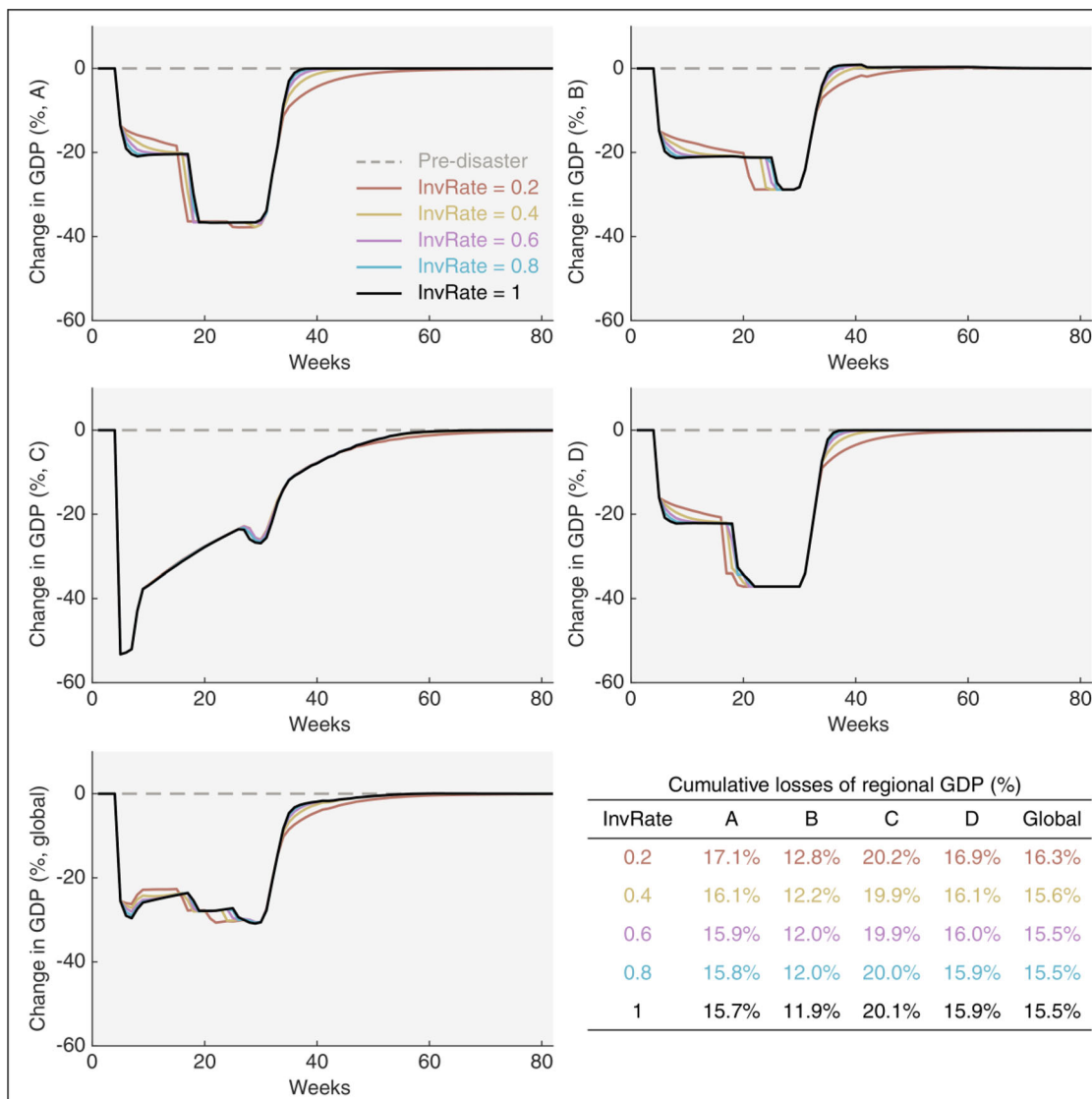


FIGURE C.4 Weekly changes in regional and global GDPs, relative to their pre-disaster levels, for the five values of inventory restoration rate, during the perfect storm of flooding, pandemic control, and export restrictions. The first four plots illustrate the robustness of results in regions A–D, respectively, and the last plot stands for the global economy. The table at the bottom right presents the cumulative losses of regional and global GDPs, relative to the pre-disaster annual levels, for the five values of inventory restoration rate.

cumulative GDP loss declines from 17.0% to 15.3% when the maximum overproduction capacity increases from 100% (no overproduction) to 150%.

Overproduction adjustment time

Here we assess the influence of the second parameter, overproduction adjustment time τ_{α} , in the overproduction module on disaster-induced economic losses. This parameter describes the time (in weeks) needed for economic sectors to achieve their maximum overproduction capacity. The results are presented in Figure C.6. Compared with the previous section, the economic losses are less sensitive to overproduction adjustment time than maximum overproduction capacity. This is consistent with the results of the sensitivity analysis in Hallegatte (2008), which concludes that the overproduction adjustment time does not matter much

in post-disaster economic recovery. Nevertheless, the economic loss in region C is still more sensitive than in other regions and shows an upward trend as the adjustment time increases. This is because the adjustment time is essentially an inverse of the adjustment speed. When sectors need more time to reach their maximum overproduction capacity, their production climbs in smaller steps each time after the shock, leading to a slower recovery and more economic losses.

A different MRIO table

In this section, we use a different MRIO table (Table B.2), which is an aggregation of the 2014 version of GTAP 10 Data Base (Aguiar et al., 2019), to construct the hypothetical global economy of four regions and five sectors and explore how our main findings will change.

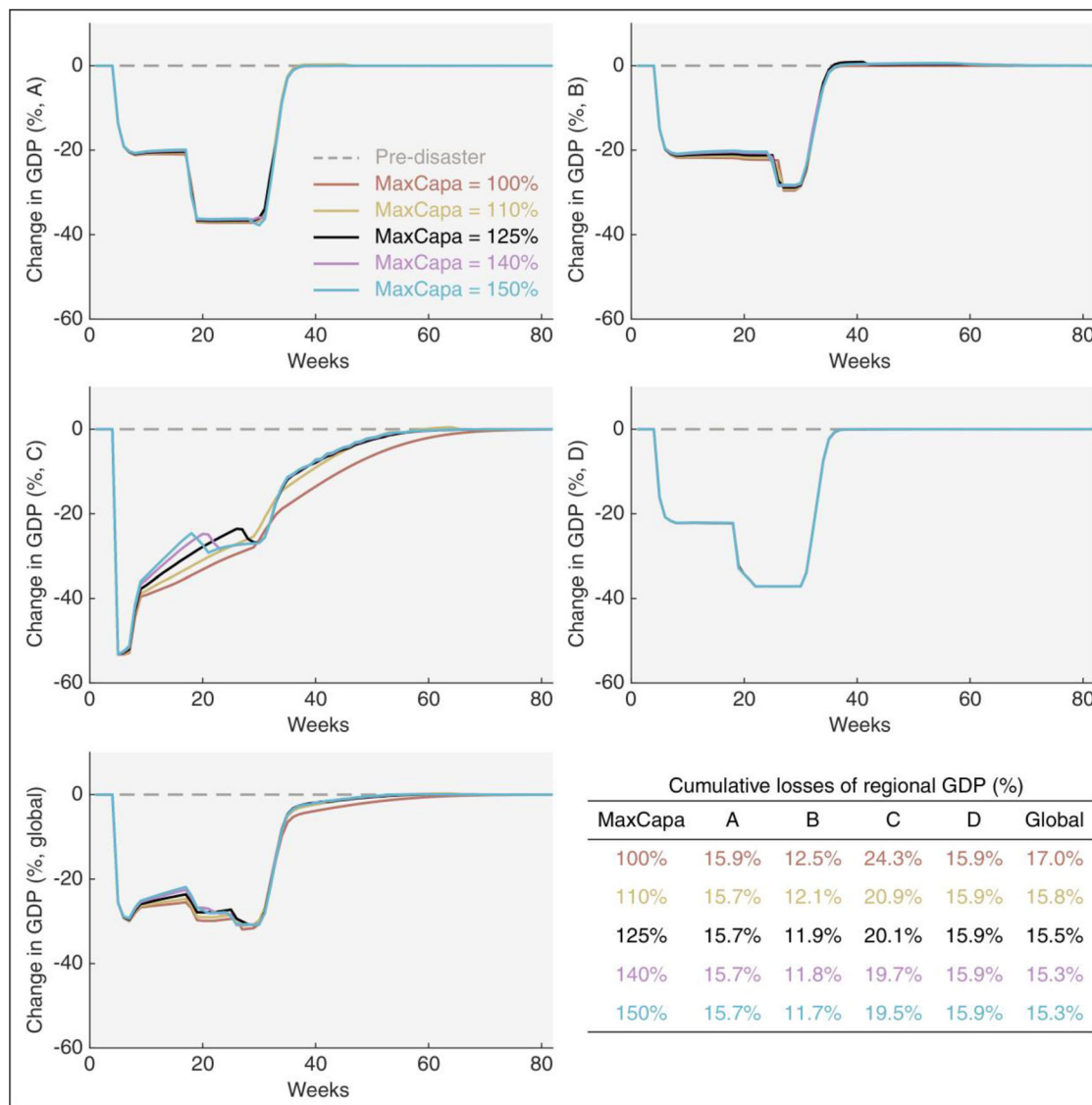


FIGURE C.5 Weekly changes in regional and global GDPs, relative to their pre-disaster levels, for the five values of maximum overproduction capacity, during the perfect storm of flooding, pandemic control, and export restrictions. The first four plots illustrate the robustness of results in regions A–D, respectively, and the last plot stands for the global economy. The table at the bottom right presents the cumulative losses of regional and global GDPs, relative to the pre-disaster annual levels, for the five values of maximum overproduction capacity.

First, we summarize the global economic losses resulting from flooding, pandemic control, and their compound, respectively, without trade restrictions for the GTAP MRIO table in Table C.3, and compare the results with Table 3 in the main text. The GTAP MRIO table results in less economic losses under the pandemic-only scenario but more than doubles the direct damage of floods at various scales. This is because the GTAP MRIO table implies a higher capital intensity in the same amount of GDP than the table used in the main text. This also incurs higher indirect losses and longer recovery time correspondingly. However, the ratios between indirect and direct impacts of flooding, ranging from 0.12 to 0.38, stay close to the results in the main text.

Besides, it is obvious from Table C.3 that similar findings on the interaction between flooding and pandemic control

(see Section 3.1.1) can be elicited with the GTAP MRIO table. On the one hand, a global pandemic control will extend the recovery time of capital damaged by flooding and therefore exacerbate its economic consequences. On the other hand, flood responses can sometimes alleviate the negative impacts of pandemic control due to the stimulus effect of post-flood reconstruction, but this only happens when the flood damage is small. If the flood damage is large enough to exceed the reconstruction stimulus, then the pandemic impacts will be aggravated.

Second, we then examine the results related to pandemic control in different flood periods with different strictness and duration. As shown in Table C.4, a pandemic control occurring after flooding leads to slightly more economic losses than it before flooding, and a stricter but shorter pandemic control is conducive to mitigate the negative impacts of the

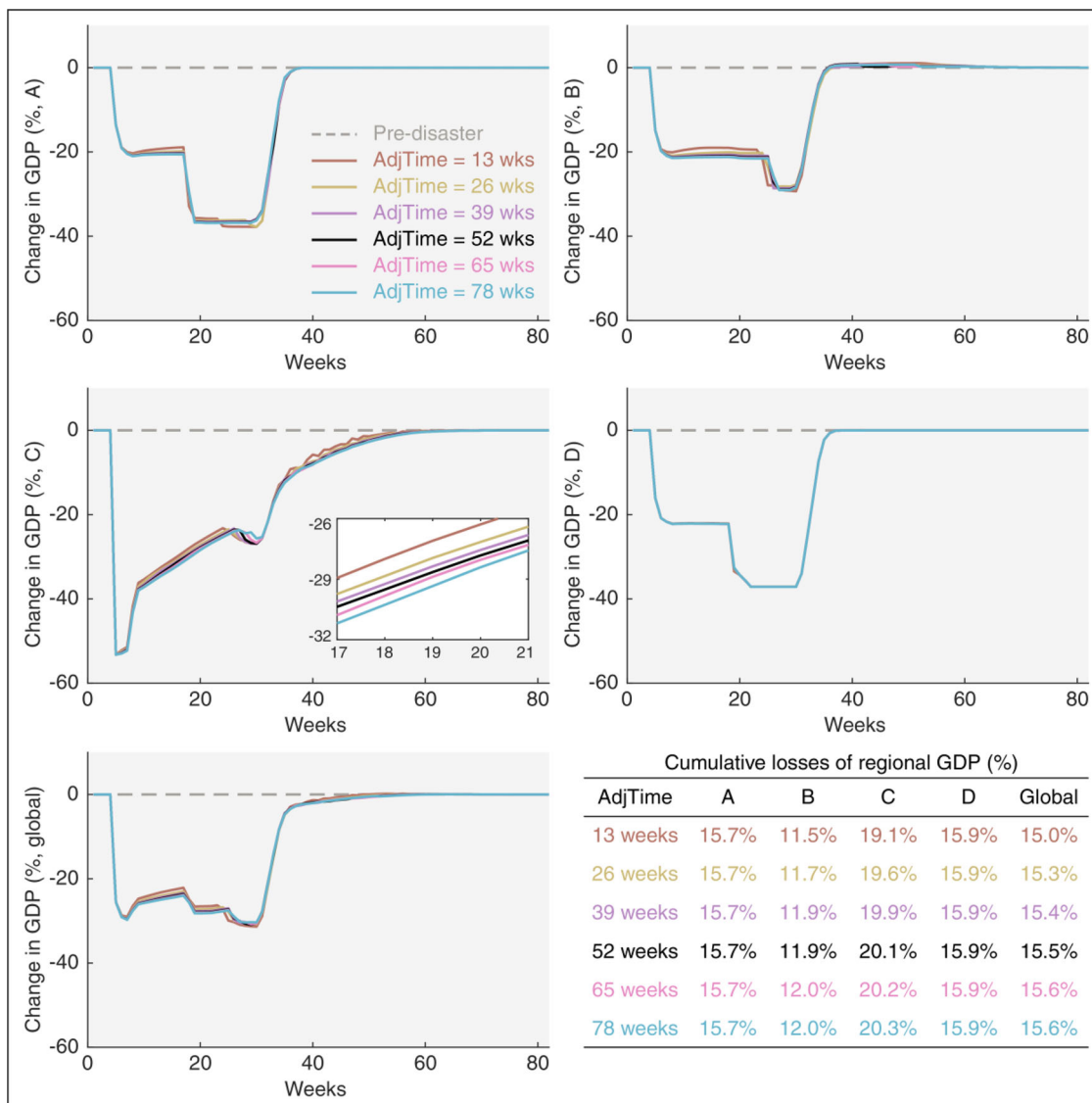


FIGURE C.6 Weekly changes in regional and global GDPs, relative to their pre-disaster levels, for the six values of overproduction adjustment time, during the perfect storm of flooding, pandemic control, and export restrictions. The first four plots illustrate the robustness of results in regions A–D, respectively, and the last plot stands for the global economy. The table at the bottom right presents the cumulative losses of regional and global GDPs, relative to the pre-disaster annual levels, for the six values of overproduction adjustment time.

TABLE C.3 Global economic footprint under the flood-only, pandemic-only, and flood + pandemic scenarios without trade restrictions for GTAP MRIO table

Scenarios	Direct damage	Indirect losses	Total impacts	Percentage of global annual GDP	Capital recovery weeks	GDP recovery weeks	
Pandemic-only	0.0	1150.2	1150.2	12.0	–	40	
Small	Flood-only	748.0	91.7	839.8	8.7	81	60
	Flood + pandemic	748.0	1138.5	1886.5	19.6	90	68
Medium	Flood-only	1496.0	386.1	1882.1	19.6	122	92
	Flood + pandemic	1496.0	1385.9	2881.9	30.0	132	100
Large	Flood-only	2244.0	852.6	3096.6	32.2	160	125
	Flood + pandemic	2244.0	1843.5	4087.5	42.5	168	131

TABLE C.4 Global indirect impacts, relative to the global annual GDP at the pre-disaster level, of the pandemic control intersecting in different flood periods with different strictness and duration for GTAP MRIO table

Scenarios		Flood scales in region C		
		Small (%)	Medium (%)	Large (%)
Global pandemic control	30%–24 control 7 weeks before flooding	11.97	14.47	19.22
	30%–24 control 7 weeks after flooding	12.14	14.62	19.36
	60%–8 control 7 weeks after flooding	10.09	12.73	17.61

TABLE C.5 Changes in cumulative GDP losses on regional and global scales by escalating export restrictions without production specialization for GTAP MRIO table^a

Scenarios		Region A (%)	Region B (%)	Region C (%)	Region D (%)	Global change (%)
Free trade		0.00	0.00	0.00	0.00	0.00
Export restriction	MANR-C	0.33	0.70	−0.08	1.18	0.53
	MANR-C, MANR-B	0.24	−0.70	1.37	0.57	0.32

^aThe cumulative GDP losses are in relative terms of the annual GDPs at the pre-disaster levels. Results in each row are the loss changes compared to the scenario of the previous row. The results are given as the ensemble mean of scenarios where different scales of floods collide with a 30%–24 pandemic control.

TABLE C.6 Changes in cumulative GDP losses on regional and global scales by escalating export restrictions with production specialization for GTAP MRIO table^a

Scenarios		Region A (%)	Region B (%)	Region C (%)	Region D (%)	Global change (%)
Free trade		0.24	0.37	0.36	0.26	0.31
Export restriction	MANR-C	14.46	17.13	2.27	15.77	12.52
	MANR-C, MANR-B	0.17	0.17	6.76	0.20	1.80

^aThe cumulative GDP losses are in relative terms of the annual GDPs at the pre-disaster levels. Results in each row are the loss changes compared to the scenario of the previous row, whereas those in the first row are compared to the free trade scenario without production specialization. The results are given as the ensemble mean of scenarios where different scales of floods collide with a 30%–24 pandemic control.

compound crises. These findings are consistent with those in Section 3.1.2 in the main text.

Third, we explore the role of export restriction in the economic footprint of a perfect storm for the GTAP MRIO table. Table C.5 presents the changes in cumulative GDP losses, both on the regional and global scales, by different export restriction scenarios without production specialization. The first row sets the free trade scenario when there are no export restrictions and thus no changes in the losses resulting from the compound crises. The second row assumes that region C imposes a 50% restriction on the exports of its “MANR” sector to “protect” its post-flood reconstruction. The results show that all regions but C suffer loss increases to various extents due to the restriction. Region C, in particular, is the only region that benefits from the restriction under all flood scales. This is because the flood-induced capital damage is large with the GTAP MRIO table at all flood scales, making the economic stimulus from the reconstruction demand outpace the negative impact of export declines. The third row presents the loss changes from the “MANR-C” restriction scenario to an escalating scenario, including B’s retaliation. This time, region C also suffers a loss increase by an average of 1.37%, which exceeds the economic gains of its own restriction and

leads to a net increase of its GDP loss by 1.29% compared to the free trade scenario. In addition, the loss of region B falls by 0.7%, back to the loss level of the free trade scenario. This may in turn enhance the motivation of region B to take retaliatory measures, which supplements the result in Section 3.2.1 in the main text.

Finally, we take into account the effect of production specialization with the presence of export restrictions. Table C.6 is similar to Table C.5, except that all scenarios are simulated under the assumption that the “MANR-B” and “MANR-C” sectors make specialized goods that cannot be substituted elsewhere. The loss changes in the first row, which reflects the role of production specialization under the free trade scenario, are obtained by comparing with the free trade scenario without production specialization (i.e., the first row in Table C.5). It is obvious that the specialization itself raises the vulnerabilities of both regional and global economies to the compound crises. From the second row, we find that the export restriction of region C on a specialized product triggers much severer economic losses to other regions, which in turn makes region C also suffer more losses through the propagation effect of the supply chains. The third row tells that the retaliation from another region and sector would trap

region C, which initiates the trade war, into further losses, and ultimately slow down the global recovery. These results are consistent with those in Section 3.2.2 in the main text.

Overall, despite higher flood-induced direct damages and stronger retaliatory motivation toward trade restrictions,

switching to the GTAP MRIO table has not changed our main findings about the economic interplay between flooding and pandemic control, or about the roles of trade restriction and production specialization in the economic footprint of a perfect storm.